2018-01-01

Influence of Mix Design Parameters on Performance of Balanced Asphalt Mixtures

Luiza Helena Barros
University of Texas at El Paso, luizahb@hotmail.com

INFLUENCE OF MIX DESIGN PARAMETERS ON PERFORMANCE OF BALANCED ASPHALT CONCRETE MIXTURES

LUIZA HELENA BARROS

Master's Program in Civil Engineering

APPROVED:

Soheil Nazarian, Ph.D., Chair

Imad Abdallah, Ph.D., Co-Chair

Ramana Chintalapalle, Ph.D.

Charles Ambler, Ph.D.
Dean of the Graduate School

Dedication

I dedicated this thesis work to my mom, Acelina Nilda Ferreira, who has been a constant source of support. Her good examples have taught me to work hard to achieve all the things I aspire.

INFLUENCE OF MIX DESIGN PARAMETERS ON PERFORMANCE OF BALANCED ASPHALT CONCRETE MIXTURES

by

LUIZA HELENA BARROS, BSCE

THESIS

Presented to the Faculty of the Graduate School of

The University of Texas at El Paso

in Partial Fulfillment

of the Requirements

for the Degree of

MASTER OF SCIENCE

Department of Civil Engineering

THE UNIVERSITY OF TEXAS AT EL PASO

August 2018

Acknowledgements

First and above all, I praise God, the almighty for providing me this opportunity and granting me the capability to proceed successfully. This thesis appears in its current form due to the assistance and guidance of several people whom I would like to offer my sincere gratitude.

I would like to express my gratitude to Dr. Soheil Nazarian and Dr. Imad Abdallah for their invaluable guidance and mentorship during my graduate course at the Center for Transportation Infrastructure Systems (CTIS). As a young civil engineering and international student they gave me the opportunity to join the research team at CTIS and acquire research experience and opportunities that cemented my passion for pavement engineering. I greatly appreciate them for allowing me the opportunity to work on of TxDOT Project 0-6923 upon which this thesis work is founded on. I would like to extend my gratitude to Robert Lee and Ryan Barborak from the Texas Department of Transportation (TxDOT) - Flexible Pavement Branch for their help and support during the research work performed under this project. Further, I would like to express my appreciation to Dr. Soheil Nazarian, Dr. Imad Abdallah, and Dr. Ramana Chintalapalle for serving as committee members for this thesis defense, and for their valuable feedback and support.

My sincere gratitude is also expressed to my supervisor Victor Garcia for his support and help during my graduate journey. His guidance was essential on my formation as a research assistant and his passion for the pavement area yielded me the drive to pursue my master's. My gratitude is also extended to the undergraduate research assistants from CTIS Angelica Torres, Getsemani Molinar, Luis Cordova, Esteban Fierro and Alexandra Torres who helped to produce the data and conduct the test methods. My deepest gratitude is also expressed to my colleagues from CTIS, Jose Garibay, Mauricio Valenzuela, Carlos Anguiano, Jose Lugo, Aaron Aceves, Denis Vieira, for the great time and support during my period at CTIS.

Abstract

With the popularity of the Balanced Mix Design (BMD) concept, the need for performance tests that can reliably evaluate the cracking and rutting potentials of asphalt concrete (AC) mixes has become more critical. A great deal of effort has been focused on incorporating test methods that can potentially improve the current AC mix-design processes and consequently screen underperforming AC mixes. However, the influence of mix design parameters on the performance of BMD mixes that provide pavement engineers and designers with thorough guidelines and a reliable and consistent test protocol has not been extensively documented.

This thesis presents an experimental evaluation of the influences of different mix design parameters on the mechanical performance of AC mixes as measured with the Overlay Tester (OT), Hamburg wheel-tracking (HWT) device, and indirect tension (IDT) tests. Superpave mixes with 12.5 mm nominal maximum aggregate size (NMAS) and asphalt binder replacement (ABR) ranging from 0% to over 50% were designed and evaluated with two different aggregate types, three neat asphalt binders with specified PG 64-22, PG 70-22 and PG 76-22, five different sources of asphalt binders with PG 64-22 and PG 70-22, three different reclaimed asphalt pavement (RAP) contents, and two sources of RAP. A performance diagram was used to interpret collectively the cracking potential, rutting potential, and tensile strength of the mixes. The coefficients of variation from the investigated parameters ranged from 0% to 20%. Given the promising results from this study, the performance test methods, analysis methodology and documented influence of mix design parameters could be potentially implemented to enhance current mix design process and design balanced AC mixes.

Table of Contents

List of Tables

List of Figures

Chapter 1: Introduction

The premature failure of asphalt concrete (AC) layers is a major concern with the performance of flexible pavements. To perform well in the field, a flexible pavement must present a balance of both crack and rut potential (Zhou et al. 2006). Premature failure is even further aggravated by the current sustainable measures such as the inclusion of reclaimed asphalt pavement (RAP), recycle asphalt shingles (RAS) and other additives. In the last decade, several highway agencies have implemented performance tests, such as the overlay tester (OT), Hamburg wheel-tracking (HWT) and indirect tension (IDT) tests, to estimate the cracking potential, rutting potential and strength of AC mixes, respectively. The implementation of these performance tests and proper analysis methodology are considered indispensable to ensure acceptable performance of mixes during the mix design and production processes.

A comprehensive mix design specification named Superior Performing Asphalt Pavements (Superpave) was developed under the Strategic Highway Research Program (Kennedy, 1994) to produce mixes with acceptable durability and compactability properties. In the Superpave mix design specifications, the anticipated performance of an AC mix is related to a target density and its volumetric properties (McDaniel and Levenberg, 2013). The rapidly increasing use of recycled materials, recycling agents, binder additives and warm mix asphalt technologies may have a significant impact on the performance of AC layers in a way that traditional volumetric mix design unaccompanied by performance tests is not applicable. In addition, results from past experimental studies have raised the question whether the Superpave volumetric mix design method alone is sufficient to ensure reliable mixture performance (Witczak et al., 2002; Bhasin et al. 2004; Valdes et al. 2010).

The ranges of recycled material, specifically RAP between 10% and 30%, are commonly used in AC mixes. McDaniel and Anderson (2001) provided preliminary guidelines for designing AC mixes with recycled materials. They recommended that a rigorous testing protocol and detailed guidelines must be implemented in order to design AC mixes with recycled materials that could provide acceptable mechanical performance. Al-Qadi et al. (2007) indicated that a lack of understanding of the aggregate and binder properties as well as gradation of RAP materials had kept the percent of RAP in AC mixes relatively low. To avoid durability and long-term performance problems related to these materials despite the recent advancements in the design of AC mixes, many State Highway Agencies (SHAs) have restrictions on the amount of recycled materials in their mixes. Therefore, the implementation of performance tests into a mix design process is paramount to ensure the optimal volumetric properties and balanced mechanical performance.

The aim of this study is to investigate the influence of several mix design parameters on the mechanical performance of AC mixes as measured with the OT, HWT and IDT tests. To achieve this objective, a parametric experimental evaluation was carried out to investigate the influence of mix design parameters including performance grade (PG) of binder, binder source, RAP content, and RAP source on the cracking and rutting potentials of AC mixes. The ultimate goal is provide performance test methods, an analysis methodology and guidelines to improve the performance of balanced AC mixes during the mix design process.

1.1 BACKGROUND

1.1.1 Superior Performing Asphalt Pavements (Superpave)

The Superpave was developed under the Strategic Highway Research Program (SHRP) to provide pavement engineers and contractors with a design tool to produce pavements that will

perform better under heavy traffic loads and extreme temperature conditions. One of the main outcome of the Superpave system is the volumetric mix design method, which is based on the assumption that performance of a mix is related to a target density and volumetric properties. The Superpave design method is divided in three phases: (1) material selection for aggregates and asphalt binder, (2) aggregate blending, and (3) analysis of volumetric properties from specimens compacted using the Superpave gyratory compactor (SGC) without complementary performance tests.

A great deal of effort has been focused toward the evaluation and implementation of performance tests to characterize the mechanical properties of AC mixes as a complement of the volumetric mix design method. According to Witczak et al. 2002, the Superpave method lacked a general strength or "push-pull" test to ensure superior performance. Bonaquist et al. (2003) suggested fundamental test methods such as the flow time, flow number, and dynamic modulus tests to evaluate the AC mix performance. Zhou et al. (2006) proposed to conduct the overlay test (OT) in conjunction with the Hamburg wheel tracking (HWT) test to balance the cracking and rutting properties of AC mixes. Al-Qadi et al. (2015) proposed a test protocol to assess the mechanical properties of AC mixes containing high recycled material content with the HWT and semi-circular bend (SCB) tests.

The Superpave mix design was developed for AC mixes containing only mineral aggregates and asphalt binders. The pavement community has focused extensively on implementing sustainable measures such as recycling previously-used materials, RAP and recycled asphalt shingles (RAS), to reduce the use of new mineral aggregates, asphalt binder and landfill space. Such approach may have an impact on the traditional volumetric mix design method. McDaniel and Anderson (2001) provided a manual for recommended use of RAP in AC

mixes using the volumetric Superpave mix design. They did not, however, suggested any performance tests after the volumetric properties of the mix design was concluded. Several studies have assessed the AC mixes containing RAP and other recycled materials using performance tests such as the indirect tension, dynamic modulus, overlay tester, permanent deformation, Hamburg wheel tracking, and semi-circular bending tests (Behnia et al., 2011; Swamy et al., 2011; Zhou et al., 2011; Al-Qadi et al., 2012). Ozer et al. (2012) studied the effect of using RAS and RAP by executing an experimental program that includes the permanent deformation, stiffness, and fracture and fatigue tests.

1.1.2 Balanced Mix Design Concept

The implementation of a balanced mix design (BMD) process has been the topic of discussion among researchers and engineers for some time. The BMD is defined by the Federal Highway Administration (FHWA) Expert Task Group (ETG) as "asphalt mix design using performance tests on appropriately conditioned specimens that address multiple modes of distress taking into consideration mix aging, traffic, climate, and location within the pavement structure" (Cox et al. 2017). The main objective of the BMD process is to balance the performance of AC mixes, especially the cracking and rutting potentials. In the last decade, several highway agencies have implemented performance tests to estimate the cracking and rutting potential of AC mixes. For instance, Texas Department of Transportation (TxDOT) incorporated the HWT test as an indicator of rutting performance, which has minimized the rutting susceptibility of AC mixes in Texas. To improve the cracking resistance of AC mixes, the OT test has been used to predict the resistance of AC mixes to cracking.

Zhou et al. (2013) suggested a balanced mix design process that consisted of the following five stages:

1. Select aggregate trial contents and asphalt binder trial contents as per traditional mix design procedure.
2. Prepare laboratory samples as per traditional mix design procedure.
3. Evaluate volumetric properties of the laboratory specimens and determine the optimum asphalt content as per traditional mix design procedure.
4. Evaluate the mixture properties (for a total of 12 laboratory specimens) using the OT (2 specimens) and HWT (2 specimens) at the optimum asphalt binder content, as well as optimum + 0.5%, and optimum + 1.0%.
5. Based on the performance data from HWT and OT requirements, select a balanced asphalt binder content. A minimum of 300 cycles and maximum of 0.5 in. rut depth were proposed for the OT and HWT tests.

1.1.3 RAP Influence on Balanced Mix Design Process

Including previously-used materials into new pavements is one way of constructing sustainable pavements. However, the BMD process should also address the proper method of incorporating RAP in the mix. A number of studies has been funded to investigate the performance of mixes containing RAP and RAS with the goal of gathering sufficient information on the performance of RAP/RAS mixes through the concept of the balanced mix design. The results from these studies have been generally mixed. While some researchers have found that the use of the recycled materials may positively influence the performance of the asphalt mixtures, others have reported that the asphalt mixtures containing recycled materials provide inferior performance when

compared with virgin mixes (Xiao et al., 2007; Tabakovíc, 2010; Behnia et al., 2011; Williams et al., 2011; Al-Qadi et al., 2012; Ozer et al., 2012).

The use of recycled materials can probably improve the performance if the rutting is the primary concern. On the other hand, if transverse cracking seems to be the main distress mechanism, the use of recycled materials needs to be controlled within certain maximum limit to not compromise the fracture properties of the AC mix (Newcomb et al., 2007; Behnia et al., 2011). Consequently, the rutting and cracking resistance of HMA mixtures containing recycled materials must be balanced during the mix design process and a proper mix design protocol is required.

1.1.4 Performance Characterization

A great deal of effort has been focused towards the evaluation and implementation of performance tests to characterize the mechanical properties of AC mixes during the mix design process (Zhou et al. 2006; Willis and Marasteanu, 2013; Al-Qadi et al., 2015; Muhunthan et al., 2017). The dynamic modulus tests has been extensively investigated due to its efficacy in delineating the performance of different mixes (Witczak et al. 2002; Carpenter 2007; Vavrik et al. 2008; Braham et al. 2011). Dynamic modulus test is conducted over a wide range of temperatures (e.g., –10°C (14°F), 4°C (39°F), 21°C (70°F), 37°C (99°F), and 55°C (131°F)) and at different frequencies (e.g., 25, 10, 5, 1, 0.5, and 0.1 Hz). The moduli obtained are used to develop a master curve. Swamy et al. (2011) and Al-Qadi et al. (2012) have found that addition of RAP can impact the dynamic modulus of AC mixes.

Permanent deformation is another mechanical property of AC mixes that is commonly determined. Two main performance tests used for the purpose of predicting susceptibility to permanent deformation (rutting) are the uniaxial flow test (AASHTO TP 79) and HWT (AASHTO T324). The flow number from uniaxial flow test is the main parameter of interest, which is the lowest rate of axial strain change for the duration of the test. In both tests the intention is to simulate

the permanent deformation caused by a cyclic load. The addition of recycled materials increases the rutting potential (Mogawaer et al. 2011; Goh and You 2011; and Al-Qadi et al. 2012). Williams (2010), through laboratory and field performance data, confirmed that the addition of recycled materials would increase rutting resistance.

The fatigue cracking is the primary concern for mixes containing recycled materials since the stiff aged binder coming from the recycled materials may accelerate the initiation and propagation of cracks. A way to measure fatigue cracking performance is using the OT test. Zhou and Scullion (2005), upgraded and standardized the OT test to determine the cracking resistance of AC mixtures by simulating the opening and closing of joints. The traditional parameter from the OT is the number of cycles required to reach a 93% load reduction. Garcia et al. (2018) proposed an analysis methodology for the OT that captured the fundamental cracking properties of the AC mixes during the initiation and propagation of a crack. They proposed two parameters to characterize the cracking properties of AC mixes under the loading conditions of the OT test, the critical fracture energy (CFE) and crack progression rate (CPR). The final evaluation of the cracking potential is carried out by cross-plotting these two indices in a design interaction plot.

1.2 STUDY METHODOLOGY AND OBJECTIVES

The main goal of this thesis is to document the influence of mix parameters on the mechanical performance of AC mixes for a balanced mix design. An extensive laboratory evaluation was carried out to document the influence of mix design parameters such as PG binder, binder source, RAP content and RAP source that may have on the cracking susceptibility and rutting potential of AC mixes. The effectiveness of the proposed tests to assess the mechanical performance of AC mixes was documented. Ultimately, this study aims to provide pavement designers and engineers with an analysis methodology and guidelines that can be used to balance

the performance of AC mixes during the design process. A flow chart of the mix design process and test protocol followed during this study is presented in Figure 1.1. Material selection consists of selecting the binder source and performance grade, aggregate source and gradation, and additives and recycled materials. The designer tries out different trial aggregate gradations that best suits the intended use and the local experience. Conducting the volumetric analysis requires the preparation of laboratory-prepared specimens utilizing a Superpave Gyratory Compactor (SGC) and evaluation of the volumetric properties of the laboratory-prepared specimens to determine OAC at the selected target density. Performance tests are incorporated to evaluate the cracking and rutting properties of the mix utilizing the OT, HWT, and IDT tests.

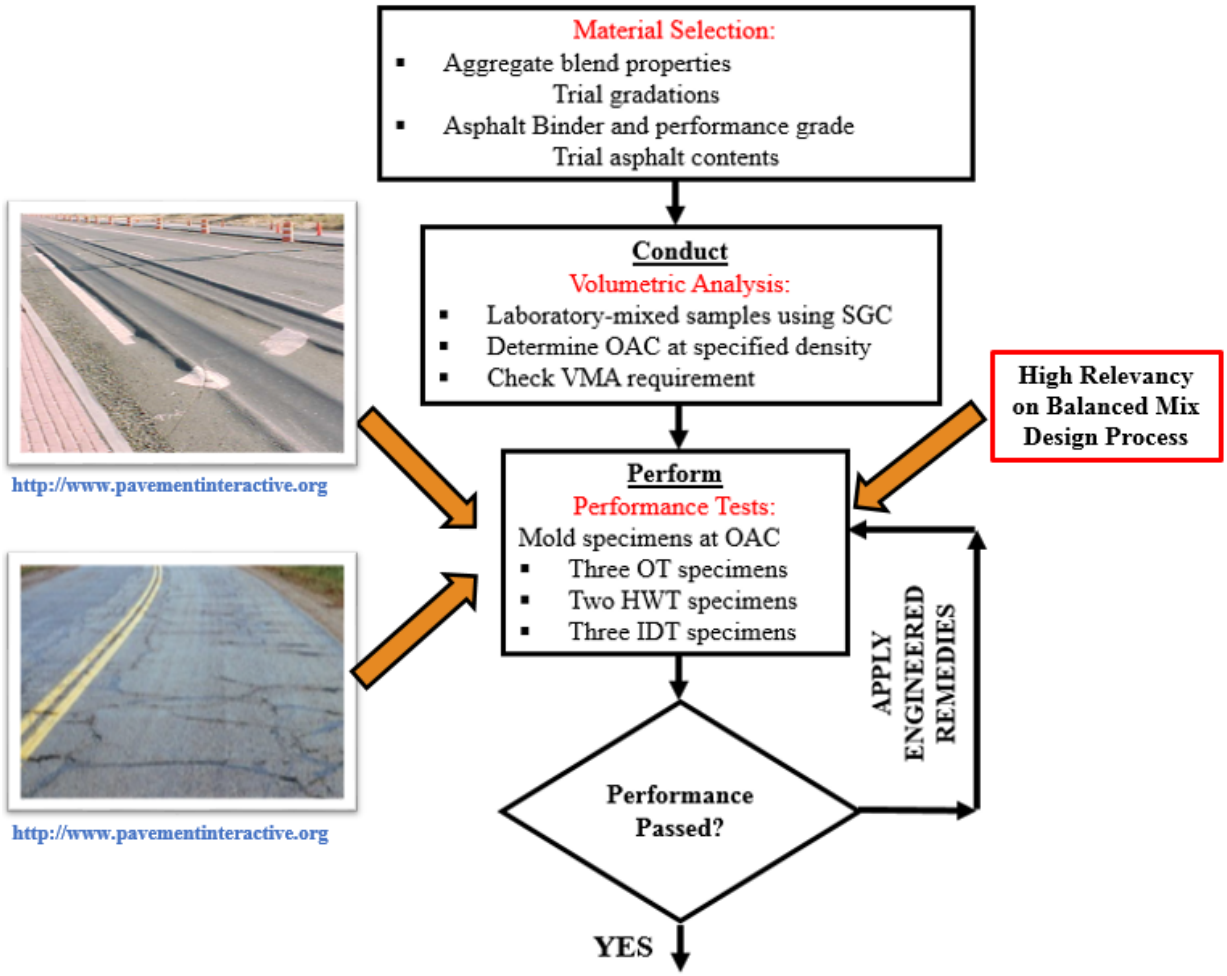

Figure 1.1 Mix Design and Testing Process

Analyzing the performance results is the final stage in determining whether the AC mix is balanced or not. For unbalanced mixes, the remedies proposed can be applied. It is paramount to evaluate the influence of mix design parameters in order to propose a balanced mix design.

To achieve the goal of the study, the technical objectives completed during this study are summarized as follow:

- Collect pavement materials (e.g. mineral aggregates, asphalt binder and recycle material) from a local asphalt mixture producer to produce several mixes. The characteristics of the selected materials were first assessed by performing sieve analysis of mineral aggregates and recycled aggregates from RAP, performance grade of asphalt binder and recycled binder from RAP, and asphalt content of RAP.
- Formulate an experiment design plan that consists of designing more than 22 different mixes utilizing the design process and volumetric analysis for Superpave mixes (ITEM 344) and carrying out several performance tests to investigate the mechanical performance of the AC mixes.
- Enhance a practical and comprehensive performance testing protocol and analysis methodology that can serve as a design tool for pavement designers and engineers during the design process of AC mixes. The OT, HWT and IDT tests were selected for the performance test protocol to determine the mechanical properties of AC mixes.
- Document the sensitivity of the proposed testing protocol and analysis methodology. Several AC mixes were designed with different aggregate types, PGs of asphalt binder, sources of binder, RAP amounts and RAP sources, and tested under the proposed testing protocol.
- Propose guidelines that provides examples of how the mix design parameters may influence the mechanical properties of AC mixes.

Chapter 2: Experiment Design Plan and Description of Pavement Materials

2.1 Introduction of Performance Test Methods

In the last decade, TxDOT implemented the OT, HWT and IDT tests to estimate the cracking, rutting and tensile strength properties of AC mixes, respectively. The test methods and procedures for the OT, HWT and IDT tests are outlined in TxDOT test procedures Tex-248-F, Tex-242-F, and Tex-226-F, respectively, and are briefly discussed next.

2.1.1 Overlay Tester (OT) Test

Detailed information of the OT test procedure is outlined in TxDOT test procedure Tex-248-F (see http://ftp.dot.state.tx.us/pub/txdot-info/cst/TMS/200-F_series/pdfs/bit248.pdf). Figure 2.1 shows the key components of an AC specimen mounted on the OT device. The OT test is conducted in a displacement control mode at a repeated loading rate of one cycle per 10 sec. The movement of the sliding platen follows a cyclic triangular waveform at a test temperature of 77ºF (25ºC). The OT specimens are nominally 6 in. (150 mm) long, 3 in. (75 mm) wide and 1.5 in. (38 mm) thick. The specimens are trimmed from the standard 6 in. (150 mm) diameter by 4.5 in. (114 mm) thick specimens compacted with a Superpave Gyratory Compactor (SGC) in accordance with test procedure Tex-241-F to a nominal target air voids of 7±1.0%.

Figure 2.1 OT Device and Specimen Setup

Garcia et al. (2018) proposed an analysis methodology that specifies the cracking properties of the AC mixes during the initiation and propagation of a crack under the loading conditions of the OT test. Figure 2.2 depicts the computation of two OT parameters, critical fracture energy (CFE, as defined in Figure 2.2a) and crack progression rate (CPR, as defined in Figure 2.2b), proposed by Garcia et al. With the new OT analysis methodology, the final evaluation of the cracking potential is carried out by cross-plotting these two indices in the design interaction plot shown in Figure 2.2c. The acceptance limits for the CPR was selected as 0.50, while the upper and lower design limits for the CFE were 3 and 1 in.-lb/in.^{2}, respectively. Garcia et al. described the rationale behind the selected acceptance limits.

The cracking characteristics of AC mixes was subjectively divided into the following four categories in Figure 2.2c:

- **Tough-Crack Resistant:** Good resistance during crack initiation (Tough) and propagation (Flexible). AC mixes with optimal cracking resistance should be in this region.
- **Tough-Crack Susceptible:** AC mixes with good resistance to crack initiation (Tough) and susceptible to crack propagation (Brittle).
- **Soft-Crack Resistant:** Susceptible to crack initiation (Soft) but good resistance against crack propagation (Flexible). AC mixes for specific application such as overlays.
- **Soft-Crack Susceptible:** AC mixes with significantly poor resistance to crack initiation and propagation.

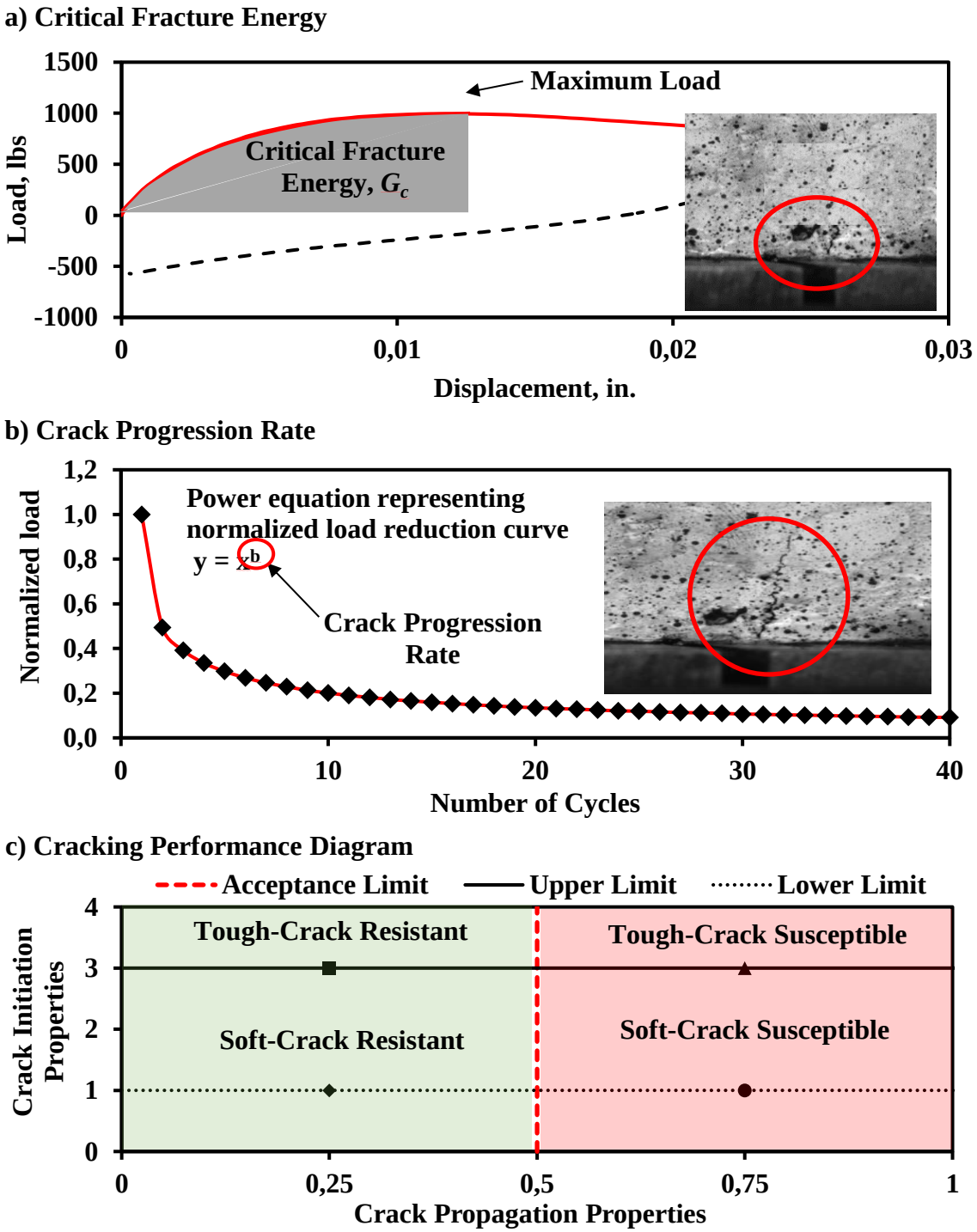

Figure 2.2 Proposed Cracking Methodology for OT Test (Garcia et al., 2018)

2.1.2 Hamburg-Wheel Tracking (HWT) Test

The HWT test method and procedure are explained in TxDOT test procedure designation Tex-242-F (see https://ftp.dot.state.tx.us/pub/txdot-info/cst/TMS/200-F_series/pdfs/bit242.pdf). The HWT test is conducted to determine the permanent deformation and moisture damage of AC mixes. Figure 2.3 depicts two sets of specimens on the HWT device. A load of 158 ± 5 lb (705 ± 22 N) is applied thru a steel wheel at 50 passes across the specimen per minute. A water bath with a temperature of 122 ± 2ºF (50 ± 1°C) is used to condition the AC specimens. The specimens are nominally 6 in. (150 mm) in diameter and 2.5 in. (62 mm) in height. A masonry saw is used to trim one end of each specimen along the edge of the mold approximately 5/8 in. (16 mm).

Figure 2.3 HWT Device and Specimen Setup

The main output parameters from the HWT test are the number of cycles and the rut depth. TxDOT requirements for the HWT test are shown in Table 2.1. These specifications will be used as a baseline to evaluate the rutting resistance of AC mixes during the course of this evaluation. Muhunthan et al. (*2017*) recommended the rutting resistance index (RRI) as an alternative performance indicator to determine the rutting potential of AC mixes. The RRI parameter is calculated using Equation 1.

$$RRI = N \times (1 - RD) \quad (1)$$

where N is the number of cycles and RD is the rut depth (in.).

The minimum RRI value was estimated for the associated PG of asphalt binder as shown in Table 2.1. For ease of use, the RRI is normalized with respect to the minimum RRI (NRRI) to discriminate among mixes with different PG binders. NRRI of unity or greater signifies an acceptable mix in terms of rutting. Equation 2 is followed to calculate NRRI.

$$NRRI = \frac{Actual\ RRI}{Minimum\ RRI\ for\ Specified\ PG} \quad (2)$$

Table 2.1 Hamburg Wheel Tracking (HWT) Test Requirements

High-Temperature Binder Performance Grade	Minimum Number of Passes	Minimum RRI
PG 64 or lower	10,000	5,100
PG 70	15,000	7,600
PG 76 or higher	20,000	10,100

PG = performance grade; RRI=rutting resistance index

2.1.3 Indirect Tensile (IDT) Test

The test method and procedure for the IDT test is outlined in TxDOT test procedure Tex-226-F (see https://ftp.dot.state.tx.us/pub/txdot-info/cst/TMS/200-F_series/pdfs/bit226.pdf), which is conducted to determine the strength of AC mixes. IDT specimens are nominally 6 in. (150 mm) in diameter and 2.5 in. (62 mm) in height. The IDT specimen is placed in an environmental controlled chamber at a temperature of 77 ºF (25 ± 1°C) for preconditioning before testing. The IDT test is a displacement-controlled test that specifies a monotonic loading rate of 50 mm/min (2 in. /min), see Figure 2.4. The tensile strength (σt) parameter is the main output from the IDT test. For an AC mix designed with any asphalt binder PG to be considered as acceptable, TxDOT

specifies a minimum and maximum tensile strength of 85 psi and 200 psi, respectively. The indirect tensile strength (ITS) parameter can be computed using Equation 3.

$$\sigma_t = \frac{2P_{max}}{\pi t D} \tag{3}$$

where P_{max} is the maximum peak load and t and D are the thickness and diameter of the IDT specimen, respectively.

Figure 2.4 IDT Test and Specimen Setup

2.1.4 Performance Diagram

Several mechanical properties should be considered to balance the performance of AC mixes. Figure 2.5 depicts the performance diagram formulated to characterize the cracking and rutting resistance of AC mixes. The crack propagation rate (CPR) from OT test is plotted on the abscissa of the performance diagram with a corresponding preliminary acceptance limit of 0.50, while NRRI from HWT test is plotted on the ordinance with an acceptance limit of 1.0. AC mixes can be preliminarily divided into the following four general categories:

Quadrant 1: Specimens prepared and tested at OAC pass both rutting and cracking resistance. Mixes with good cracking resistance (flexible) and rutting resistance (rigid) are expected to be in this quadrant.

Quadrant 2: Specimens prepared and tested at OAC pass only the rutting resistance requirements. AC mixes with poor cracking resistance (brittle) and high rutting resistance (rigid).

Quadrant 3: Specimens prepared and tested at OAC only pass the cracking resistance requirements. AC mixes with acceptable cracking resistance (flexible) but poor rutting resistance (unstable).

Quadrant 4: Specimens prepared and tested at OAC fails both rutting and cracking resistance requirements. AC mixes with significantly poor cracking resistance (brittle) and rutting resistance (unstable).

In addition, tensile strength is shown as a data label for a more comprehensive analysis of the AC mixes. Any AC mix with properties that plots within the green shaded area in Figure 2.5 and exhibits a minimum tensile strength of 85 psi is considered acceptable. The performance diagram will provide a three dimensional analyses of the mechanical properties of AC mixes that includes the cracking, rutting and stiffness properties of the AC mixes.

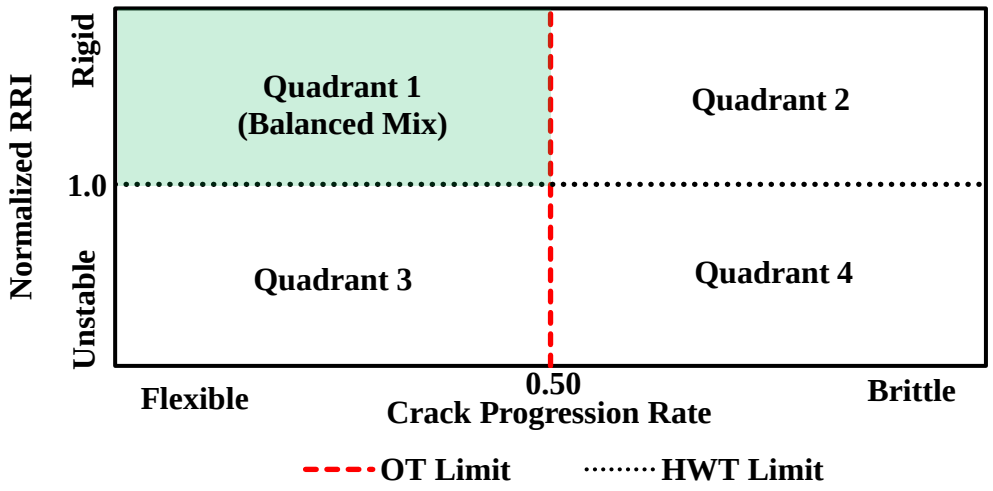

Figure 2.5 Performance Diagram for Balance AC Mixes

2.2 DESCRIPTION OF PAVEMENT MATERIALS

A number of AC mixes were designed to investigate the influence of several mix design parameters throughout an extensive laboratory evaluation and characterization program. AC mixes were designed with two different aggregate types and three neat asphalt binders with specified PG 64-22, PG 70-22 and PG 76-22, five different sources of asphalt binders with PG 64-22 and PG 70-22, three different RAP contents, and two sources of RAP. The mix type was a Superpave Type C (SP C) mix design with a nominal maximum aggregate size (NMAS) of 12.5 mm (ITEM 344). The experiment design plan was divided into four general categories based on the mix design variables evaluated:

Category 1, ***influence of binder PG,*** consists of six AC mixes. Three different PG asphalt binders (PG64-22, PG 70-22 and PG76-22) were used with two different aggregates (dolomite and granite). In this case the asphalt source and gradation were maintained the same.

Category 2, ***influence of asphalt binder source***, consists of ten AC mixes. Asphalt binders with PG 64-22 and PG 70-22 from five different sources were used with only dolomite aggregates. In this case the aggregate type and gradation were maintained the same.

Category 3, ***influence of RAP content***, consists of eight AC mixes. Four different RAP contents (0%, 15%, 30% and 45%) were used with two different aggregates (dolomite and granite). In this case the asphalt source and gradation were maintained the same.

Category 4, ***influence of RAP source***, consists of six AC mixes. Three different RAP contents (15%, 30% and 45%) were used with one type of aggregates (dolomite) and two sources of RAP. In this case the asphalt source and gradation were maintained the same.

The AC mixes were designed with a Superpave gyratory compactor to meet a 96% target density at 50 gyrations (N_{design}) and an angle of gyration of 1.25˚ in accordance with Tex-241-F. The amount of material necessary to obtain a standard specimen height of 115 ± 5mm (4.5 ± 0.2 in.) was about 4850 g (10.7 lb) for dolomite and 4600 g (10.1 lb) for granite. The optimum asphalt content (OAC) was determined as the asphalt content required to achieve 4.0% air voids at N_{design}. OAC values ranged from 4.1% to 6.2%.

2.2.1 Characterization of Aggregate Sources

The sampled aggregates consisted of a dolomite and a granite aggregate with surface aggregate classification (SAC) of B and A, respectively. Detailed information about the aggregate types and properties is summarized in Table 2.2. The particle size distribution of the aggregates and RAP materials from washed sieve analysis were obtained as per Test Procedure Tex-200-F. The materials were then combined to obtain the master aggregate gradation shown in Figure 2.6. That master gradation, which complied with TxDOT SP-C (ITEM 344) gradation, was maintained constant for all experiments. For the mixes containing RAP, the gradation of the RAP was kept constant according to its respective RAP sieve analysis while the gradation of the aggregates was adjusted to produce a similar final aggregate gradation. The gradations for the virgin aggregates for the three RAP contents and the two RAP sources can be found in Appendix A.

Table 2.2 Aggregate types and Properties

Parameter	Aggregate Type	
	Dolomite	Granite
Los Angeles Abrasion	27	28
Source Soundness Magnesium	3	14
Source Micro-Deval	11	10
Source Acid Insoluble	0	94
Aggregate Crushing Value, %	25	21
Aggregate Impact Value, %	27	28

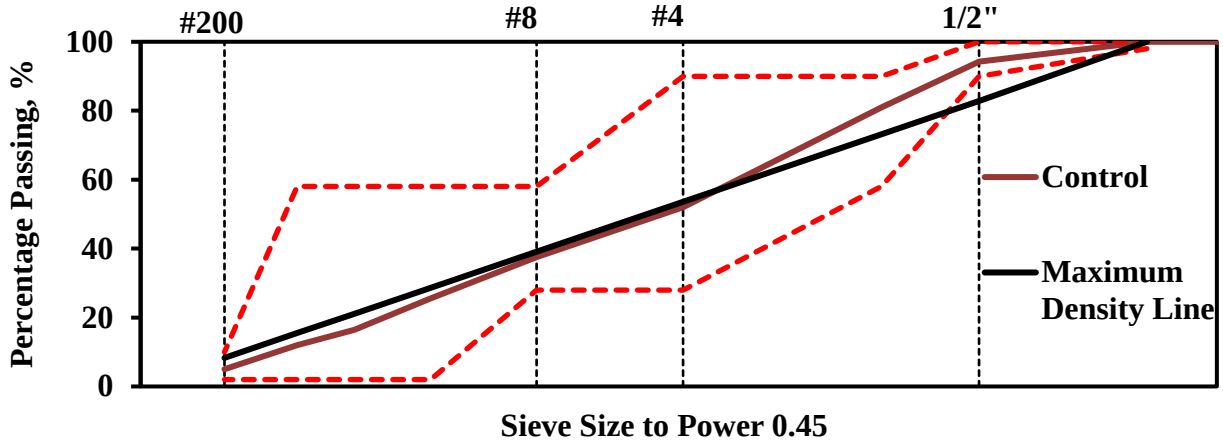

Figure 2.6 SP-C Master Aggregate Gradation with 12.5 mm NMAS

2.2.2 Characterization of Asphalt Binder

A total of three different PG asphalt binders were used for this study. Furthermore, for PG's 64-22 and 70-22 a total of asphalt from five different sources were analyzed. The high true PG, and low true PG were obtained for all original asphalt binders, as shown in Table 2.3.

Table 2.3 Performance Grading of Asphalt Binders

PG	Source	True High PG (°C)	True Low PG (°C)	Specified PG
64-22	A	68.3	-24.8	64-22
	B	67.9	-24.6	64-22
	C	69.1	-26.1	64-22
	D	66.6	-25.2	64-22
	E	67.2	-25.7	64-22
70-22	A	72.8	-25.9	70-22
	B	69.0	-26.1	64-22
	C	76.1	-26.3	76-22
	D	75.3	-26.2	70-22
	E	74.2	-25.4	70-22
76-22	A	70.6	-28.3	70-28

2.2.3 Characterization of Reclaimed Asphalt Pavement (RAP) Materials

Two sources of RAP material were selected and included in the experiment design plan for this study. The asphalt content of RAP was estimated using an ignition oven as described in Tex-236-F (see ftp://ftp.dot.state.tx.us/pub/txdot-info/cst/TMS/200-F_series/pdfs/bit236.pdf). The

average asphalt contents for RAP Source A and RAP Source B from four random samples were 5.4% and 5.5%, respectively. These values were taken into account for the reduction of virgin asphalt added during the mix design.

The particle size distribution of the RAP material was determined following the washed sieve analysis as per test procedure Tex-200-F. Figure 2.7 shows that the gradation from the two RAP sources are slightly different. As mentioned previously, the gradation of RAP was kept constant as the washed sieve analysis while the gradation of the virgin aggregates was adjusted to produce a similar master gradation.

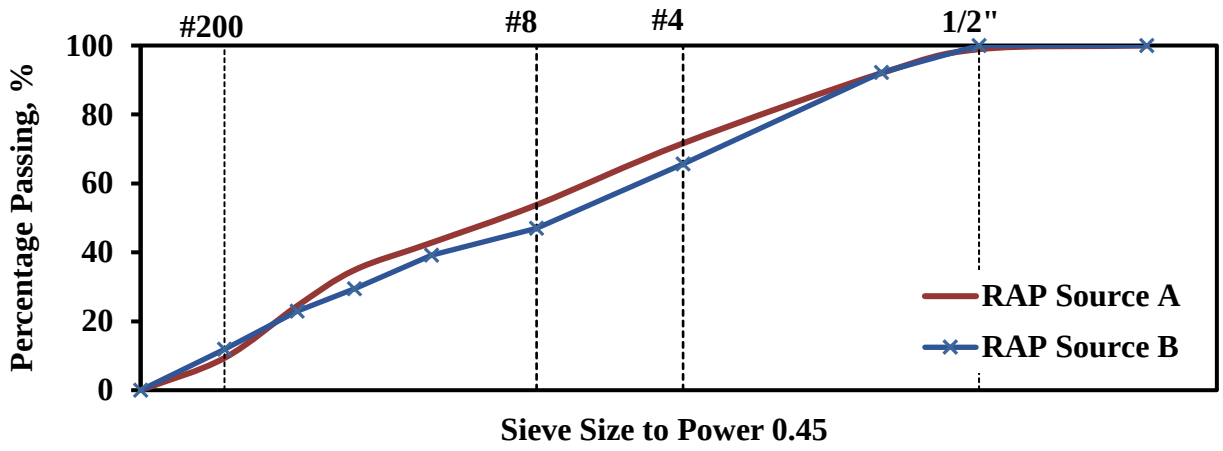

Figure 2.7 RAP Average Aggregate Gradation from Washed Sieve analysis

The high temperature true grade was obtained from Dynamic Shear Rheometer (DSR) as per test procedure AASHTO T 315 and the low temperature true grade was obtained from Bending Beam Rheometer (BBR) as per AASHTO T 313. Original high temperature true grade obtained from the recycled binder was 82.8 C° for RAP Source A and 90.5 C° for RAP Source B. The low temperature true grade was -19.9 C° for RAP source A and -27.9 C° for RAP Source B.

Chapter 3: Thorough Evaluation of AC Mix Design Parameters

The influence of mix design parameters was documented by characterizing the mechanical performance of AC mixes with the OT, HWT and IDT test methods. Triplicate specimens were tested for the OT and IDT tests to account for the repeatability of the test results, while only one set of HWT specimens was tested. Statistical parameters such as average, standard deviation, and coefficient of variation (COV) were calculated to determine the consistency of the test results. The results from the evaluation of AC mix design parameters and test methods are discussed next.

3.1 Influence of Performance Grade of Asphalt Binders on AC Mix Performance

3.1.1 Volumetric Properties

The influence of the PG of the asphalt binder was investigated using PG 64-22, PG 70-22 and PG 76-22 binders from the same source (Source A). AC mixes were designed with the selected asphalt binders and using 100% virgin aggregates from both aggregate sources (e.g. dolomite and granite). The volumetric properties, such as OAC, voids in mineral aggregate (VMA), voids filled with asphalt (VFA) and dust-to-binder ratio of the AC mixes are summarized in Table 3.1. For each aggregate source, OACs did not change appreciably (less than 0.3%) for different binders. The mixes containing granite aggregates yielded about 1% higher OAC. VMAs ranged from 13.6% to 14.4% for dolomite and 15.9% to 16.1% for granite. Since the minimum VMA requirement is 15% for SP-C mixes, the AC mixes designed with dolomite aggregates did not meet the minimum requirement. The VFAs fell in a narrow range of 70.6% to 75.2%. TxDOT does not have a requirement for VFA. However, according to AASHTO M 323, these values are from 70 to 80 for ESALs[a] (in millions) smaller than 0.3. All mixes yielded similar dust-to-binder ratios that fell within the recommended limits, which is from 0.6 to 1.6.

Table 3.1 Volumetric Properties of AC Mixes: Asphalt Binder PG

Aggregate Type	Designation	OAC, %	VMA, %	VFA, %	Dust/ Asphalt Ratio
Dolomite	64-22	4.4	14.4	72.2	1.10
	70-22	4.3	14.2	71.8	1.20
	76-22	4.1	13.6	70.6	1.20
Granite	64-22	5.4	16.1	75.2	0.90
	70-22	5.3	16.0	75.0	0.90
	76-22	5.3	15.9	74.8	0.90

3.1.2 Mechanical Performance

The results from OT tests of the dolomite and granite aggregates are presented in Figure 3.1. The error bars in the figures depict ±1 standard deviation. The COV values were less than 11% and 8% for CFE and CPR, respectively. All AC mixes with virgin aggregates but different binder PGs are within the acceptable zone of the interaction plots. The increase in high-temperature grade of the binder increased CFE and decreased (improved) CPR, regardless of the aggregate type. This means that the increase in the high-temperature grade of the binder would make the mix tougher during the initiation of the crack and more flexible during the propagation of the crack.

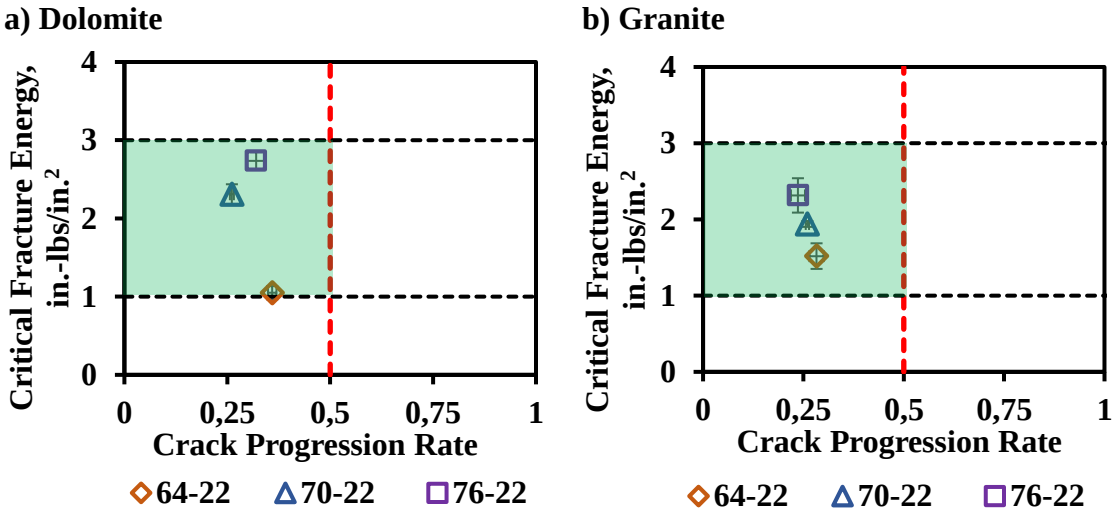

Figure 3.1 Crack Interaction Plot for Cracking Resistance: Asphalt Binder PG

The HWT test results are presented in Figure 3.2. The data labels represents NRRI. Increasing the high-temperature grade of the binder resulted in mixes with better rutting resistance. AC mixes designed with granite aggregates yielded higher RRI. Based on NRRI, all AC mixes exhibited acceptable rutting resistance regardless of their asphalt binder PG.

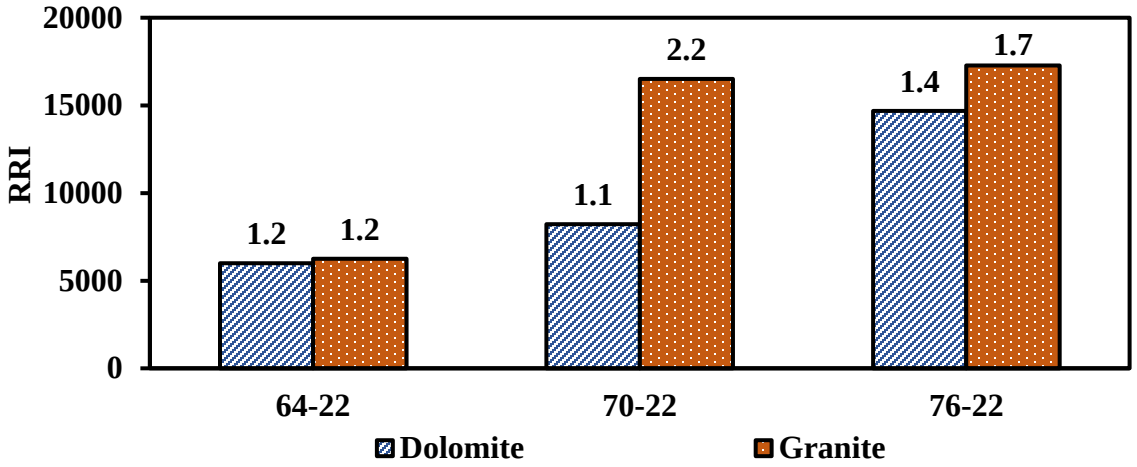

Figure 3.2 HWT Test Results for AC Mixes: Asphalt Binder PG

The average tensile strengths are presented in Figure 3.3. COV for each AC mix is included as a data label to consider the consistency of the IDT test results. The COV values ranged from 3% to 6%. As the high-temperature grade of the binder increases, the tensile strength of the AC mixes increases as well. Unlike the other performance tests, the IDT strengths of the mixes with different aggregate types but the same binder grade are similar. The lower and upper specification limits of 85 psi and 200 psi, respectively, are also included in the figure. All mixes, except for mixes with PG 64-22 binder, exceed the lower limit.

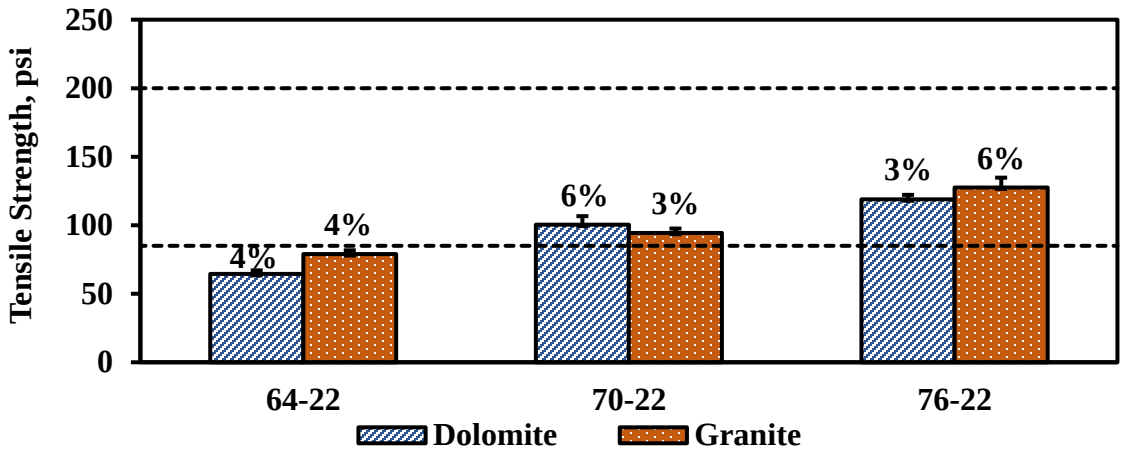

Figure 3.3 IDT Test Results for AC Mixes: Asphalt Binder PG

3.1.3 Performance Diagram of AC Mixes

The results from the OT, HWT and IDT tests are presented in the performance diagram of Figure 3.4. The mixes with dolomite and granite aggregates are represented with hollowed and solid markers, respectively. The AC mixes located within the green area are considered balanced in terms of cracking and rutting. The tensile strengths of the AC mixes, which is presented as a data label, are acceptable except for the two mixes with PG 64-22 (highlighted in red). The AC mixes with A70-22 and A76-22 can be classified as balanced. However, the AC mixes containing dolomite aggregates exhibited VMAs that are less than the minimum VMA requirements. A summary of the tests results is presented in Table 3.2.

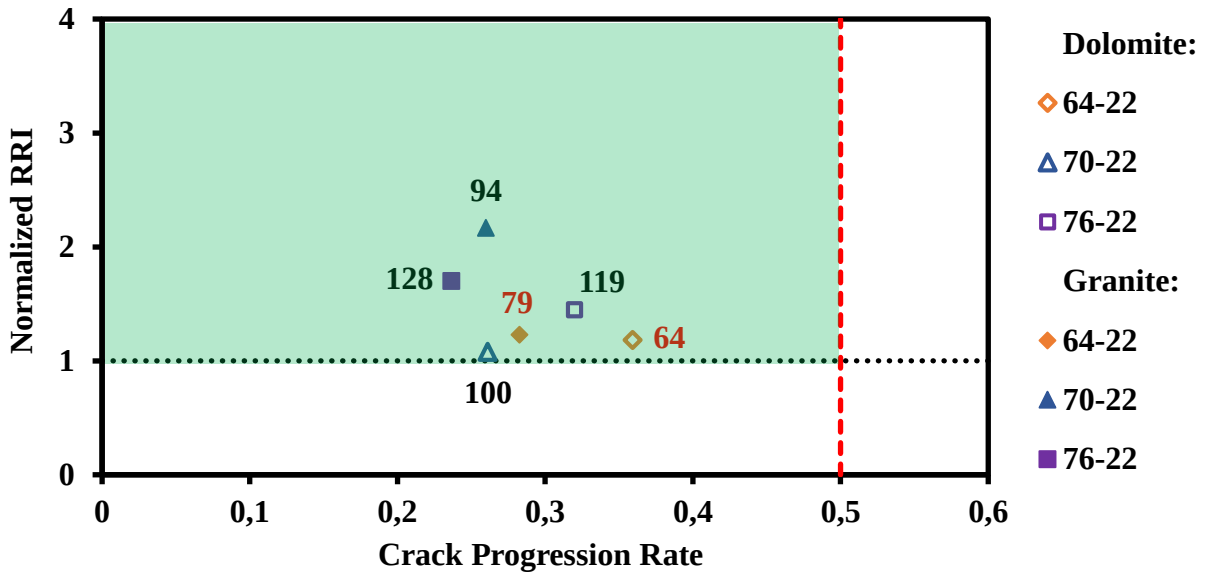

Figure 3.4 Performance Diagram for Balanced AC Mixes: Asphalt Binder PG

Table 3.2 Summary of Performance Test Results for AC Mixes: Asphalt Binder PG

Performance Parameters			Dolomite			Granite		
			PG 64-22	PG 70-22	PG 76-22	PG 64-22	PG 70-22	PG 76-22
OT	CFE, in.-lbs/in.²	Avg.	1.0	2.3	2.7	1.5	1.9	2.3
		COV	8%	6%	4%	11%	2%	10%
	CPR	Avg.	0.36	0.26	0.32	0.28	0.26	0.24
		COV	3%	2%	8%	6%	2%	7%
HWT	RRI	RRI	6003	8218	14685	6248	16512	17268
		NRRI	1.2	1.1	1.4	1.2	2.2	1.7
IDT	Tensile Strength, psi	Avg.	64	100	119	79	94	128
		COV	4%	6%	3%	4%	3%	6%

3.2 Influence of Asphalt Binder Source on AC Mix Performance

3.2.1 Volumetric Properties

The influence of the asphalt binder source was investigated by acquiring PG 64-22 and PG 70-22 from five different producers. The AC mixes were designed with dolomite aggregates only. The volumetric properties of the AC mixes were estimated and are summarized in Table 3.3. The OACs varied narrowly between 4.2% and 4.5%, with an average of about 4.4%. The VMA and

VFA ranged from 13.8% to 14.6% and 71.0% to 72.6%, respectively. None of the AC mixes meet the minimum VMA requirements of 15% for SP-C mixes. The AC mixes yielded similar dust-to-binder ratios that are within the recommended limits of 0.6 to 1.6.

Table 3.3 Volumetric Properties of AC Mixes: Asphalt Binder Source

Binder Type	Producer Code	OAC, %	VMA, %	VFA, %	Dust/ Asphalt Ratio
PG 64-22	A	4.4	14.4	72.2	1.10
	B	4.3	14.1	71.6	1.20
	C	4.4	14.3	72.0	1.10
	D	4.4	14.3	72.0	1.10
	E	4.5	14.6	72.6	1.10
PG 70-22	A	4.3	14.2	71.8	1.20
	B	4.2	13.8	71.0	1.20
	C	4.5	14.5	72.4	1.10
	D	4.2	13.9	71.2	1.20
	E	4.4	14.3	72.0	1.10

3.2.2 Mechanical Performance

The OT results from all AC mixes are presented in the cracking interaction plot of Figure 3.5. The error bars represent ±1 standard deviation. The COV values were less than 18% and 16% for CFE and CPR, respectively. All AC mixes exhibited acceptable cracking resistance as judged by the CFE and CPR parameters, except for mix with PG 70-22 binder form Source B that did not meet the minimum CFE. In the contrary to the mixes with PG 64-22, the five sources of PG 70-22 yield mixes with considerably different CFE values ranging from 0.6 to 2.7 in.-lbs/in.^{2}. The consistency in the OT test results from the AC mixes with different PG 64-22 asphalt binders can be expected since these binders are not modified. On the other hand, the differences in CFE for AC mixes with PG 70-22 can be attributed to different modifications that are applied to asphalt binders in order to meet the requirements of that binder grade.

The HWT test results are presented in Figure 3.6. NRRI is reflected as a label above each bar. AC mixes with different PG 64-22 binders yielded RRI values that ranged from 3429 to 8644. Asphalt binder from Source A and Source D yielded marginally acceptable performance. Mixes from Source B and Source C yielded did not pass the minimum TxDOT requirement.

The range of RRI values for AC mixes with different PG 70-22 binders varied significantly. AC mixes made with binders from Source C and Source D exhibited acceptable with NNRI values of 1.9 and 2.1, respectively. The AC mix with Source A yielded a marginally acceptable performance. AC mixes from Source B and Source E yielded NRRI values equal to 0.5, indicating that they are rut susceptible. This study demonstrates the significant impact that the source of the binder, especially for the modified asphalt binders, has on the performance of a given AC mix.

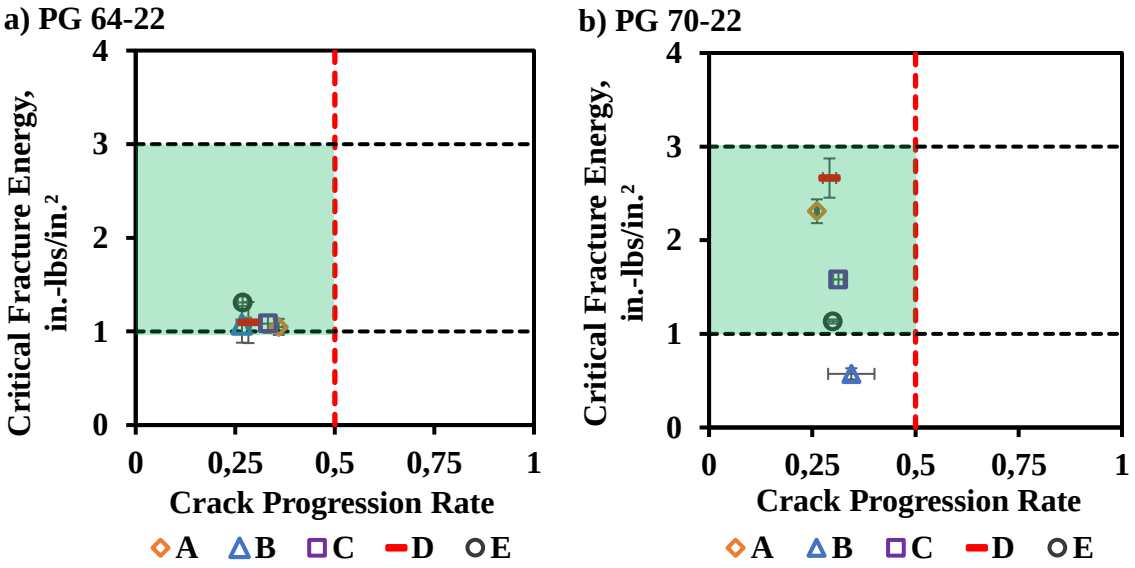

Figure 3.5 Crack Interaction Plot for Cracking Resistance: Asphalt Binder Source

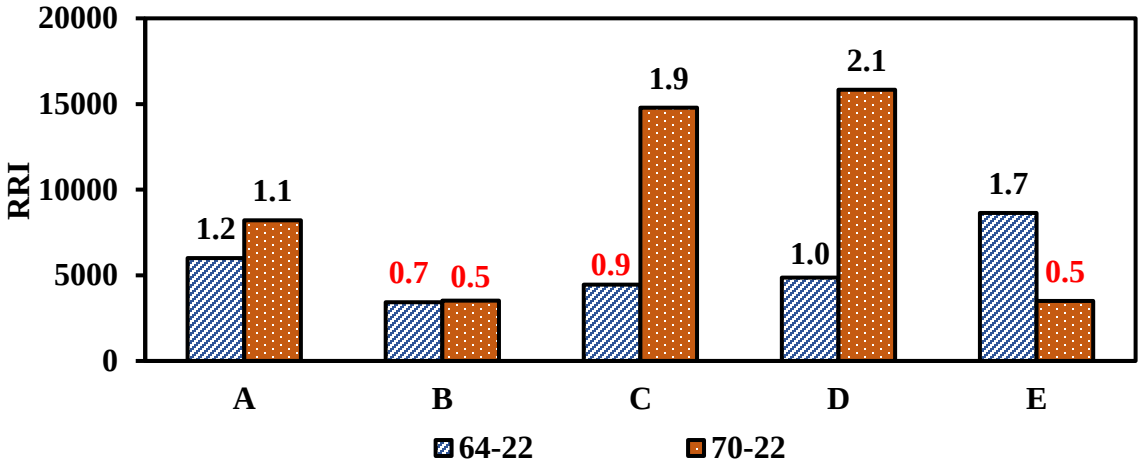

Figure 3.6 HWT Test Results for AC Mixes: Asphalt Binder Source

The average tensile strengths from the ten AC mixes are presented in Figure 3.7. The COVs that are shown as data labels are less than 6%. None of the AC mixes with PG 64-22 binder achieved the minimum required tensile strength of 85 psi. The tensile strengths for only three of the AC mixes with PG 70-22 binders were greater than 85 psi.

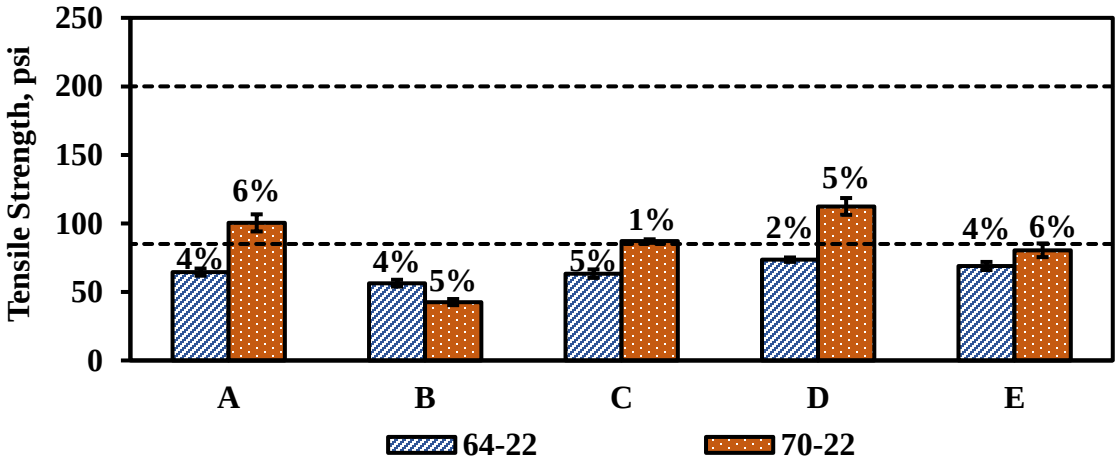

Figure 3.7 IDT Test Results for AC Mixes: Asphalt Binder Source

3.2.3 Performance Diagram of AC Mixes

A summary of the test results from this portion of the study is presented in Table 3.4. The OT, HWT and IDT performance indicators are superimposed on the performance diagram shown in Figure 3.8. In general, the AC mixes with PG 64-22 asphalt binders did not meet the minimum

required tensile strengths. Only three AC mixes (those from Sources A, C and D) with PG 70-22 exhibited balanced performance.

Table 3.4 Summary of Performance Test Results for AC Mixes: Asphalt Binder Source

Performance Parameters			PG 64-22 Binder from Source					PG 70-22 Binder from Source				
			A	B	C	D	E	A	B	C	D	E
OT	CFE, in.-lbs/in.²	Avg.	1.0	1.1	1.1	1.1	1.3	2.3	0.6	1.6	2.7	1.1
		COV	8%	18%	8%	20%	5%	6%	10%	5%	8%	2%
	CPR	Avg.	0.36	0.27	0.33	0.28	0.27	0.26	0.34	0.31	0.29	0.30
		COV	3%	5%	5%	2%	4%	2%	16%	4%	6%	4%
HWT	RRI	RRI	6003	3429	4459	4873	8644	8218	3526	14787	15835	3501
		NRRI	1.2	0.7	0.9	1.0	1.7	1.1	0.5	1.9	2.1	0.5
IDT	Tensile Strength, psi	Avg.	64	56	63	74	69	100	43	87	112	80
		COV	4%	4%	5%	2%	4%	6%	5%	1%	5%	6%

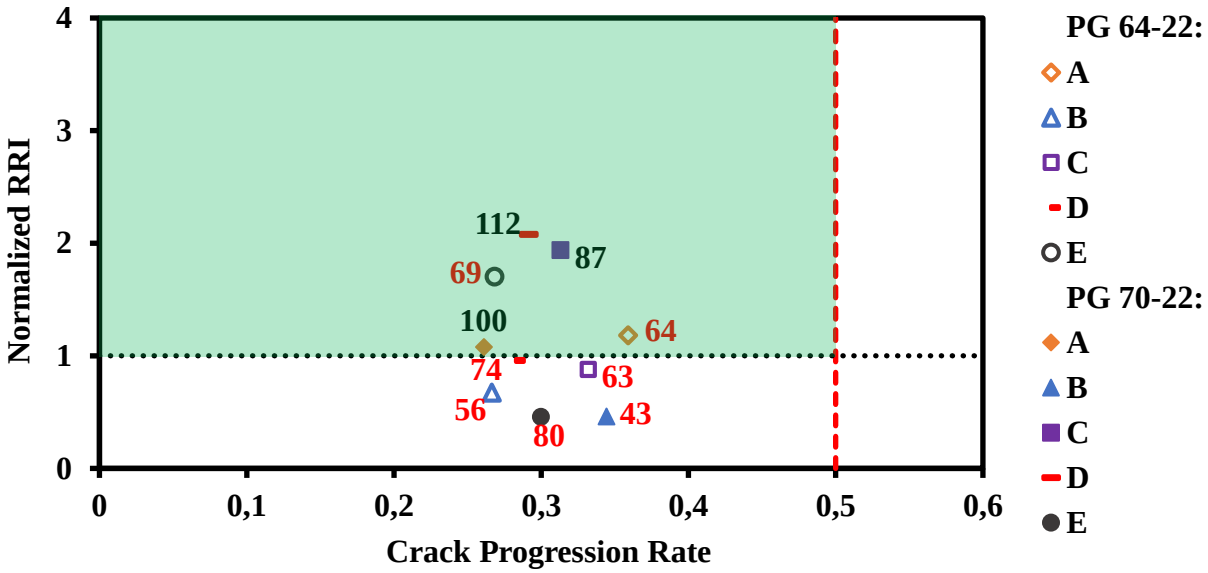

Figure 3.8 Performance Diagram for Balanced AC Mixes: Asphalt Binder Source

3.3 INFLUENCE OF RECLAIMED ASPHALT PAVEMENT CONTENT ON AC MIX PERFORMANCE

3.3.1 Volumetric Properties

Three different RAP contents of 15%, 30% and 45% were considered for this purpose in addition to the control cases (i.e., no RAP). AC mixes were designed with the PG 64-22 binder from Source A, and both aggregate types, dolomite and granite. Each of the six AC mixes with RAP were designed individually.

The volumetric properties of the AC mixes are summarized in Table 3.5. Similar OAC values were obtained for AC mixes containing up to 30% RAP. Significantly higher OACs were obtained for AC mixes with 45% RAP. The minimum VMA of 15% for SP-C mixes could not be achieved for dolomite mixes with no RAP and 15% RAP.

Table 3.5 Volumetric Properties of AC Mixes Changing RAP Content

Aggregate Type	RAP Content	OAC, %	ABR, %	VMA, %	VFA, %	Dust/ Asphalt Ratio
Dolomite	None	4.4	0	14.4	72.2	1.10
	15%	4.7	17.2	14.9	73.2	1.10
	30%	4.7	34.7	15.1	73.5	1.10
	45%	5.8	42.5	17.5	77.1	0.80
Granite	None	5.4	0	16.1	75.2	0.90
	15%	5.3	15.3	16.0	75.0	0.90
	30%	5.6	29.1	16.7	76.0	0.90
	45%	6.2	39.8	18.1	77.9	0.80

3.3.2 Mechanical Performance

The OT test results are presented in the crack interaction plot of Figure 3.9. The COV values were less than 17% and 14% for CFE and CPR, respectively. CFE increased with the increase in RAP content for AC mixes with both dolomite and granite aggregates. The mixes containing 45% RAP yielded the highest CFE, while those without RAP yielded the lowest. The AC mixes with different RAP contents yielded similar CPR values. The good cracking resistance

of AC mixes containing 45% RAP can be explained by the increased in OAC during the design process.

The HWT test results are presented in Figure 3.10. The NRRI values, which are shown as labels above data points, was calculated using the minimum RRI value required for PG 64-22. As such, a PG bump was not assumed for the AC mixes designed with 15% RAP or more to be consistent during the analysis of the test results. All AC mixes meet the minimum performance requirements for HWT tests. The addition of RAP improved considerably the rutting resistance of the AC mixes.

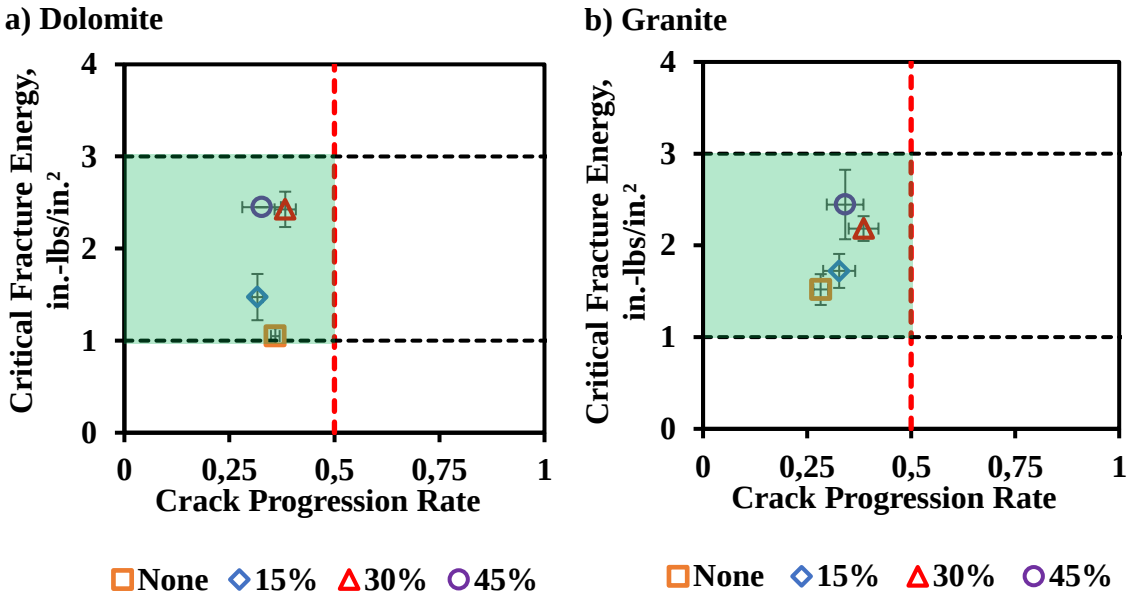

Figure 3.9 Crack Interaction Plot for Cracking Resistance: RAP Content

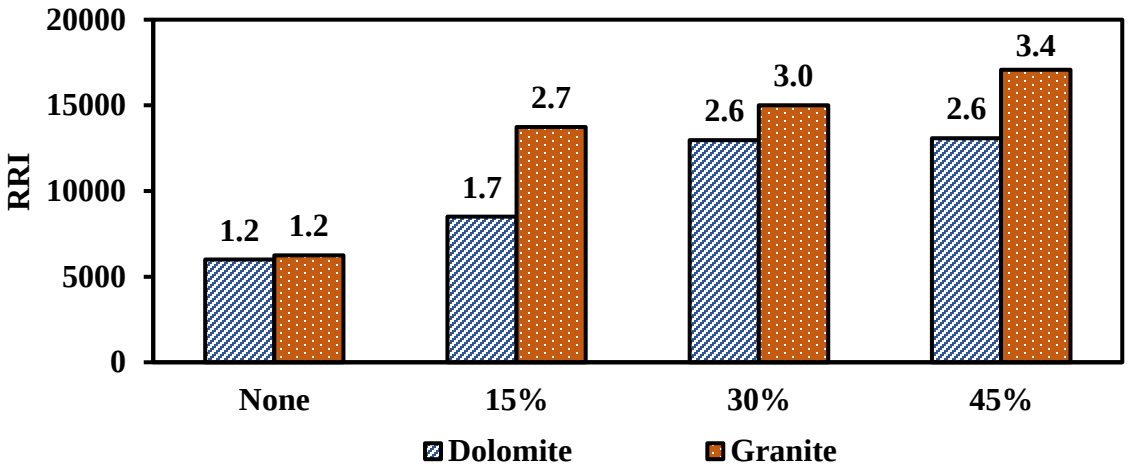

Figure 3.10 HWT Test Results for AC Mixes: RAP Content

The average IDT test results are presented in Figure 3.11. The COVs that are shown as data labels are less than 5%. The tensile strengths for all AC mixes, except for the AC mixes designed with 0% RAP met the minimum required value. Increasing the RAP content increased the tensile strength of the AC mixes. The tensile strengths for AC mixes with 45% RAP were similar or less than those with 30% RAP, due to a higher OAC obtained during the design process.

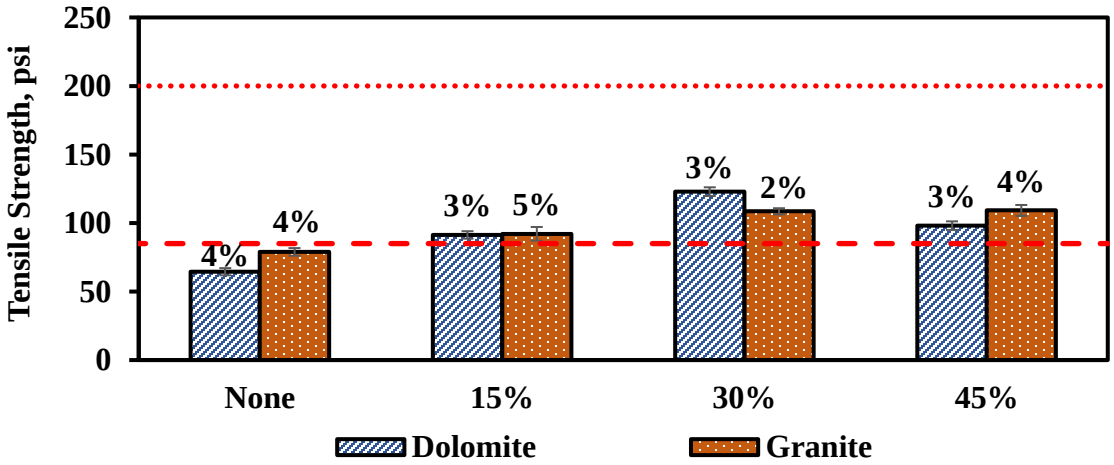

Figure 3.11 IDT Test Results for AC Mixes: RAP Content

3.3.3 Performance Diagram of AC Mixes

A summary of the test results is presented in Table 3.6. The results from the OT, HWT and IDT tests are superimposed on the performance diagram shown in Figure 3.12. Most AC mixes

performed well in cracking and rutting resistance. Both AC mixes without RAP did not meet the minimum required tensile strength, even though they performed satisfactorily in OT and HWT tests. All AC mixes with RAP in this study can be categorized as balanced. However, the AC mix with dolomite aggregates and 15% RAP strictly met the minimum VMA requirement.

Table 3.6 Summary of Performance Test Results for AC Mixes: RAP Content

Performance Parameters			Dolomite				Granite			
			0% RAP	15% RAP	30% RAP	45% RAP	0% RAP	15% RAP	30% RAP	45% RAP
OT	CFE,in.-lbs/in.²	Avg.	1.0	1.5	2.4	2.4	1.5	1.7	2.2	2.4
		COV	8%	17%	8%	N/A	11%	11%	6%	15%
	CPR	Avg.	0.36	0.32	0.38	0.33	0.28	0.33	0.39	0.34
		COV	3%	4%	7%	14%	6%	12%	9%	13%
HWT	RRI	RRI	6003	8501	12969	13071	6248	13724	15008	17071
		NRRI	1.2	1.7	2.6	2.6	1.2	2.7	3.0	3.4
IDT	Tensile Strength, psi	Avg.	64	91	123	98	79	92	109	109
		COV	4%	3%	3%	3%	4%	5%	2%	4%

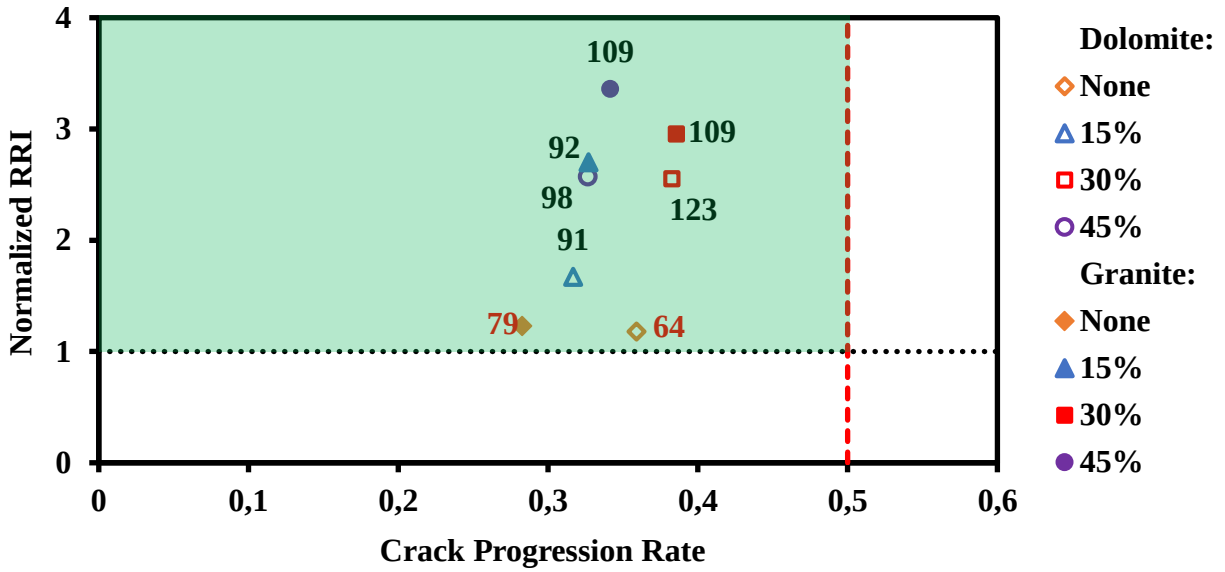

Figure 3.12 Performance Diagram for Balanced AC Mixes: Asphalt Binder Source

3.4 Influence of Reclaimed Asphalt Pavement Source on AC Mix Performance

3.4.1 Volumetric Properties

AC mixes were designed with RAP material from two different sources. Three different RAP contents of 15%, 30% and 45% were considered in addition to the control case (i.e., no RAP). The PG 64-22 binder from Source A was used with both RAP sources. Each of the six AC mixes with RAP were designed individually. The volumetric properties of the AC mixes are summarized in Table 3.7. Similar OAC values were obtained for AC mixes containing up to 30% RAP. Significantly higher OACs were obtained for AC mixes with 45% RAP. The minimum VMA of 15% for SP-C mixes could not be achieved for source A mixes with 15% RAP and for source B mixes with 15% and 30%.

Table 3.7 Volumetric Properties of AC Mixes Changing RAP Source

RAP Source	RAP Content	OAC, %	ABR, %	VMA, %	VFA, %	Dust/ Asphalt Ratio
None	None	4.4	0.0	14.4	72.2	1.10
A	15%	4.7	17.2	14.9	73.2	1.10
	30%	4.7	34.7	15.1	73.5	1.10
	45%	5.8	42.5	17.5	77.1	0.80
B	15%	4.3	18.8	14.0	71.4	1.20
	30%	4.2	40.1	14.0	71.4	1.20
	45%	4.8	52.7	15.1	73.5	1.10

3.4.2 Mechanical Performance

The OT test results are presented in the crack interaction plot of Figure 3.13. The COV values were less than 20% and 14% for CFE and CPR, respectively. CFE increased with the increase in RAP content for AC mixes with both RAP sources. The AC mixes containing 45% RAP yielded the highest CFE, while those without RAP yielded the lowest. The AC mixes with different RAP content yielded similar CPR values for Source A. The AC mixes with RAP from

source B yielded an increase of CPR with the increase of RAP content. The good cracking resistance of AC mix containing 45% RAP from source A can be explained by the higher OAC obtained during the mix design process.

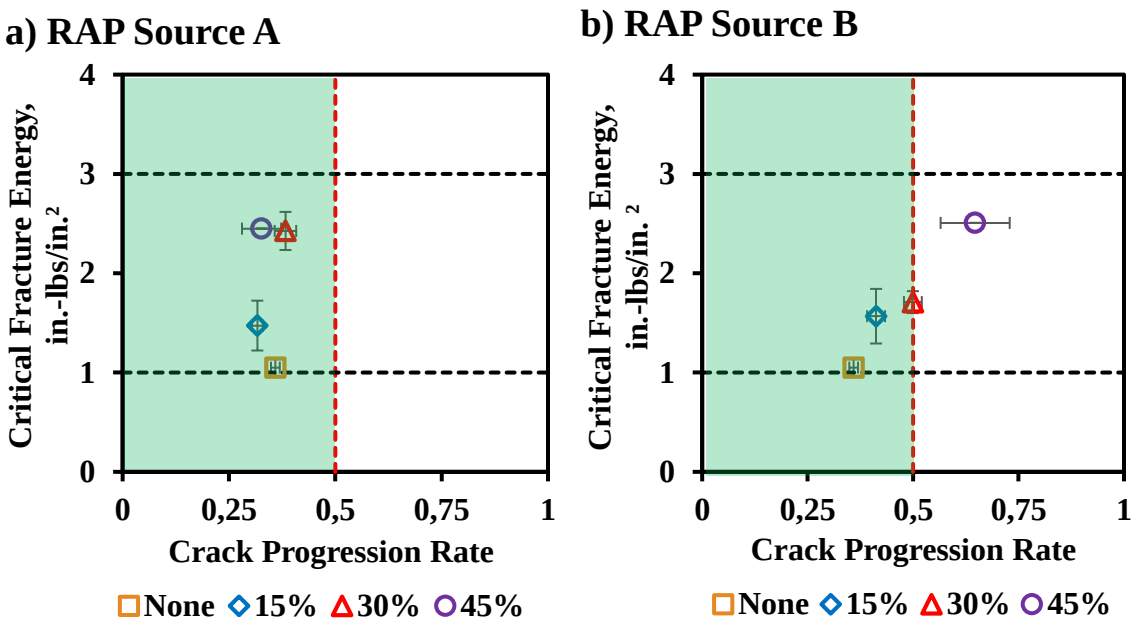

Figure 3.13 Crack Interaction Plot for Cracking Resistance: RAP Source

The HWT test results are presented in Figure 3.14. The NRRI values, which are shown as labels above data points, was calculated using the minimum RRI value required for PG 64-22. As such, a PG bump was not assumed for the AC mixes designed with 15% RAP or more to be consistent during the analysis of the test results. All AC mixes meet the minimum performance requirements for HWT tests. The addition of RAP improved considerably the rutting resistance of the AC mixes for both RAP sources.

The average IDT test results are presented in Figure 3.15. COVs are presented as data labels and were less than 7%. The tensile strengths for all mixes, except for the AC mixes designed with 0% RAP met the minimum required value. Increasing the RAP content increased the tensile

strength of the AC mixes. The tensile strength for mix with 45% RAP was less than that with 30% RAP on source A, due to a higher OAC obtained during the design process.

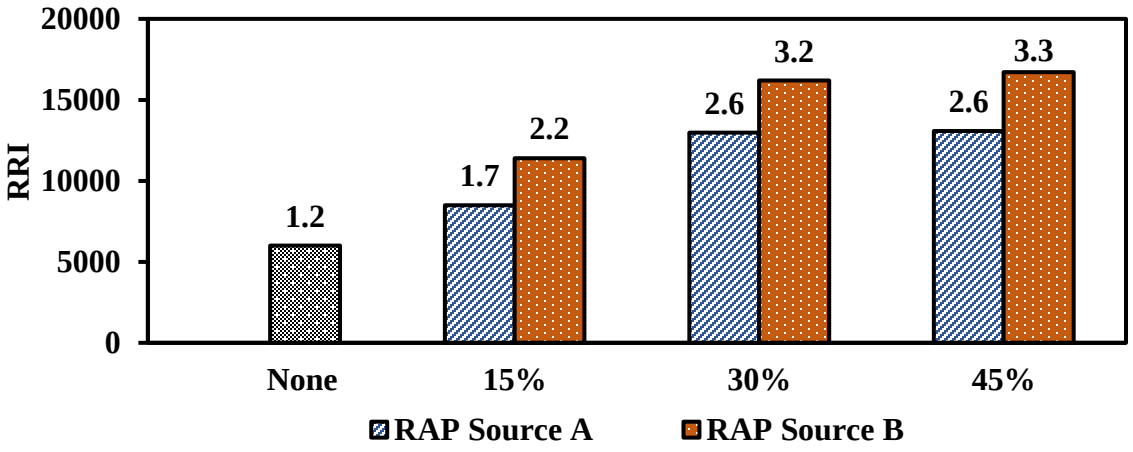

Figure 3.14 HWT Test Results for AC Mixes: RAP Source

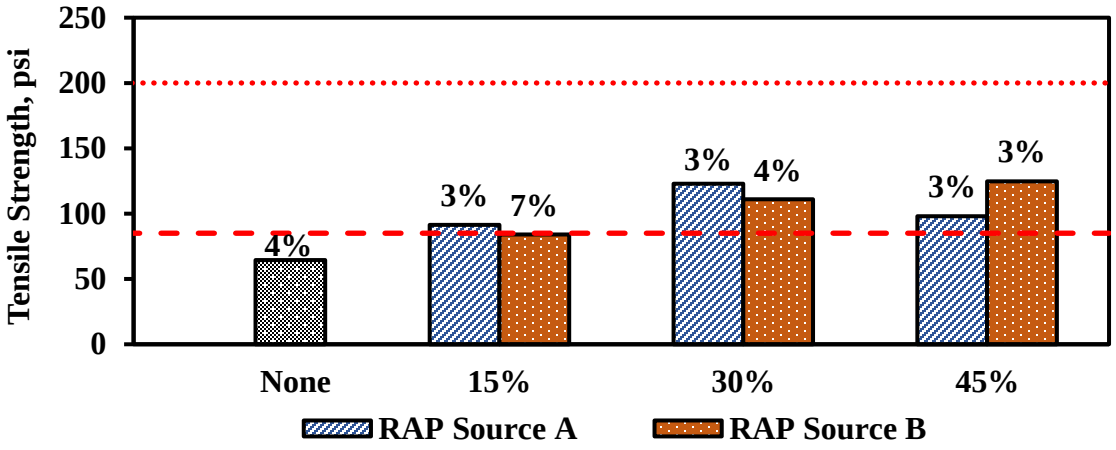

Figure 3.15 IDT Test Results for AC Mixes: RAP Source

3.4.3 Performance Diagram of AC Mixes

A summary of the test results is presented in Table 3.8. The results from the OT, HWT and IDT tests are presented in the performance diagram of Figure 3.16. The AC mixes with RAP from source A and B are represented with hollowed and solid markers, respectively. The AC mixes located within the green area are considered balanced in terms of cracking and rutting. The tensile strengths of the AC mixes, which is presented as a data label, are acceptable except for the AC

mix with 0% RAP (highlighted in red). All AC mixes with RAP from source A in this study can be categorized as balanced. However, the 15% RAP strictly met the minimum VMA requirement. From source B, the only mix categorized as balanced is the 15% RAP. However, it exhibited a VMA that is less than the minimum VMA requirement.

Table 3.8 Summary of Performance Test Results for AC Mixes: RAP Source

Performance Parameter			None	Source A			Source B		
				15% RAP	30% RAP	45% RAP	15% RAP	30% RAP	45% RAP
OT	CFE, in.-lbs/in.²	Avg.	1.0	1.5	2.4	2.4	1.6	1.7	2.5
		COV	8%	17%	8%	0%	18%	6%	0%
	CPR	Avg.	0.36	0.32	0.38	0.33	0.41	0.50	0.65
		COV	3%	4%	7%	14%	9%	4%	13%
HWT	RRI	RRI	6003	8501	12969	13071	11394	16189	16709
		NRRI	1.2	1.7	2.6	2.6	2.2	3.2	3.3
IDT	Tensile Strength, psi	Avg.	64	91	123	98	84	111	125
		COV	4%	3%	3%	3%	7%	4%	3%

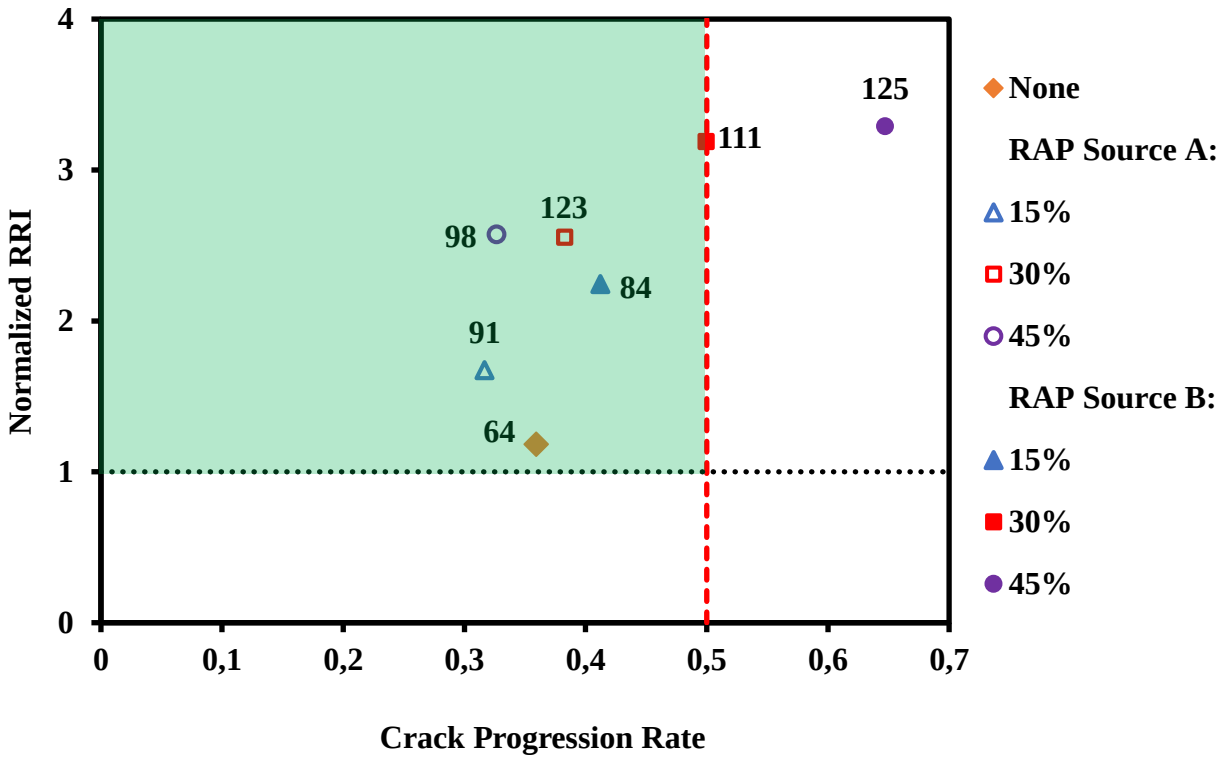

Figure 3.16 Performance Diagram for Balanced AC Mixes: RAP Source

Chapter 4: Conclusions and Recommendation

4.1 Conclusions and Key Findings

The influence of mix design variables such as PG, binder source, RAP content, and RAP source on the cracking resistance, rutting resistance and tensile strength of AC mixes was documented to provide recommendations for effectively designing balanced AC mixes. The mechanical performance of AC mixes was investigated with an analysis methodology that uses the parameters from the OT, HWT and IDT test methods. The documented influence from the mix design parameters were utilized to develop guidelines that can help to balance the mechanical performance of AC mixes during the mix design process.

From this study, the following conclusions were drawn:

1. An analysis methodology that incorporates the OT, HWT and IDT tests and corresponding performance indicators seemed to be promising in screening and discriminating the performance of AC mixes.
2. The selected performance test methods showed acceptable repeatability. The OT test results, based on CPR and CFE parameters, presented a maximum COV value of 18%. A maximum COV of 5% was obtained for the tensile strength from the IDT tests. The low variability of the proposed performance indices allows to reliably implement the performance diagram of CPR, NRRI and tensile strength.
3. The increase in high-temperature grade of the binder improved CFE and CPR parameters from OT tests, resulting in a tougher and more flexible mix during the crack initiation and propagation phases, respectively. In addition, the increase in high-temperature grade of the binder resulted in more rut-resistant mixes with higher tensile strength as determined with the HWT and IDT tests, respectively. In general, as the high-temperature grade increased,

the cracking, rutting and tensile properties of the AC mixes evaluated in this study improved as long as individual mix design was carried out.

4. The influence of binder source was different for asphalt binders with PG 64-22 and 70-22. Mixes with PG 64-22 binders from five sources exhibited similar cracking performance. The change of source for asphalt binders PG 70-22 changed significantly CFE from OT tests, while CPR values remained similar. Similar patterns were observed for HWT and IDT results. The binder properties of PG 70-22 binders must be further investigated since the OT, HWT and IDT tests results revealed a significant variation of the results among binders from different sources.
5. The increase in RAP content led to an increase in the CFE from OT tests, resulting in a more rigid and less flexible mix during the crack initiation and propagation phases, respectively. In addition, the increase in RAP resulted in more rut-resistant mixes with higher tensile strength as determined with the HWT and IDT tests, respectively.
6. The influence of RAP source was different for AC mixes with RAP from source A and B. Mixes with RAP from source A presented good cracking resistance, tensile strength, and rutting resistance. On the other hand, mixes with RAP from source B improved the rutting of the AC mixes but impacted negatively the cracking resistance of mixes above 15% RAP.

From this study, guidelines that provides examples of how the mix design parameters may influence the mechanical properties of AC mixes are provided as shown in Figure 4.1. The proposed remedies are summarized:

1. If the problem is only low CFE, a bump of binder PG or an increase of RAP content may solve the problem. On the other hand, if the problem is only high CFE, a decrease of binder PG or a decrease of RAP content may solve the problem.

2. If the CPR is marginal, reducing the RAP content may solve the problem, especially when dealing with a RAP source of high true PG.
3. If the problem is only a low RRI, a bump of binder PG or an increase of RAP content may solve the problem. In addition, the asphalt binder source should not be discarded on this case, especially when dealing with a modified binder.
4. If the problem is only a low ITS, a bump of binder PG or an increase of RAP content may solve the problem. In addition, the binder source should not be discarded on this case.

4.2 RECOMMENDATIONS

The following recommendations are provided to continue evaluating and implementing the proposed test protocols for balanced mixes:

1. One of the challenges of this study is to establish reliably the acceptance limits and boundaries for the four quadrants from the balanced performance diagram. A larger testing matrix should be executed to gather more performance data and delineate potential OT, IDT and HWT test results' thresholds.
2. An extensive testing matrix that includes AC mixes with poor cracking resistance or rutting resistance should be executed to gather more performance data and help delineate potential test results' thresholds.
3. Evaluation of other mix design parameters such as aggregate properties and gradation should be considered for an extensive analysis of mix design parameters influence on the mechanical performance of AC mixes.
4. Guidelines should be established so that the pavement engineer and designer can improve the performance of poor performing mixes utilizing the performance diagram and proposed test methods.

PARAMETER	FEATURES	VOL	CFE	CPR	RRI	ITS
RAP Amount ↑	Dolomite RAP Source1	↔	↑	↔	↑	↑
	Granite RAP Source1	↔	↑	↔	↑	↑
PG Grade ↑	Dolomite	↔	↑	↔	↑	↑
	Granite	↔	↑	↔	↑	↑
Binder Source ≠	Dolomite 64-22	↔	↔	↔	≠	↔
	Dolomite 70-22	↔	≠	↔	≠	≠
RAP Source ↑	Dolomite RAP Source1	↔	↑	↔	↑	↑
	ELP Dolomite RAP Source 2	↔	↑	↑	↑	↑

Figure 4.1 Guidelines for Balancing AC Mixes

References

1. Al-Qadi, I. L., Ozer, H., Lambros, J., El Khatib, A., Singhvi, P., Khan, T., & Doll, B. 2015. Testing Protocols to Ensure Performance of High Asphalt Binder Replacement Mixes Using RAP and RAS. Illinois Center for Transportation/Illinois Department of Transportation.

2. Al-Qadi, I. L., Q. Aurangzeb, and S. H. Carpenter. 2012. Impact of High RAP Contents on Structural and Performance Properties of Asphalt Mixtures. Report No. FHWA-ICT-12-002. Illinois Center for Transportation, Rantoul, IL.

3. Al-Qadi, L. I., M. Elseifi, and H. S. Carpenter. March 2007. Reclaimed Asphalt Pavement – A Literature Review. Publication FHWA-ICT-07-001, Illinois Center of Transportation.

4. Behnia, B., E. Dave, S. Ahmed, W. Buttlar, and H. Reis. 2011. Effects of recycled asphalt pavement amounts on low-temperature cracking performance of asphalt mixtures using acoustic emissions. Transportation Research Record: Journal of the Transportation Research Board, Vol. 2208, pp. 64–71.

5. Bhasin, A., Button, J., & Chowdhury, A. 2004. Evaluation of simple performance tests on hot-mix asphalt mixtures from south central United States. Transportation Research Record: Journal of the Transportation Research Board. 174-181. F

6. Cox, B. C., Smith, B. T., Howard, I. L., & James, R. S. 2017. State of knowledge for Cantabro testing of dense graded asphalt. Journal of Materials in Civil Engineering, 29(10), 04017174.

7. D. Newcomb, E. R. Brown, and J. A. Epps. 2007. Quality Improvement Series 124: Designing HMA Mixtures with High RAP Content: A Practical Guide, National Asphalt Pavement Association, Lanham, Maryland.

8. F. Zhou, S. Hu, X. Hu, G. Das, and T. Scullion. November 2011. High RAP Mix Design Methodology with Balanced Performance, Research Report FHWA/TX-11/0-6092-2, Texas Transportation Institute, College Station, Texas.

9. Garcia, V., Miramontes, A., Garibay, J., Abdallah, I., and Nazarian, S. 2018. Assessing Crack Susceptibility of Asphalt Concrete Mixtures with Overlay Tester. Journal of Testing and Evaluation 46(3).

10. Goh, S. W., and Z. You. 2011. Evaluation of recycled asphalt shingles in hot mix asphalt. In Proceedings of the 1st Congress of the Transportation and Development Institute of ASCE, pp. 638–645. Washington, DC: American Society of Civil Engineers.

11. Kennedy, T. W., G. A. Huber, E. T. Harrigan, R. J. Cominsky, C. S. Hughes, H. Von Quintus, and J. S. Moulthrop. 1994. Superior Performing Asphalt Pavements (Superpave®). The Product of the SHRP Asphalt Research Program. SHRP-A-410. TRB, National Research Council, Washington, D.C.

12. McDaniel, R. S., and E. Levenberg. 2013. Risk Management of Low Air Void Asphalt Concrete Mixtures. Publication FHWA/IN/JTRP-2013/15. Joint Transportation Research Program, Indiana Department of Transportation and Purdue University, West Lafayette, Indiana, https://doi.org/10.5703/1288284315217

13. McDaniel, R., and Anderson, R.M. 2001.Recommended Use of Reclaimed Asphalt Pavement in the Superpave Mix Design Method: Technician's Manual. NCHRP Report 452. Washington, D.C.

14. Mogawer, W., A. Austerman, R. Bonaquist, and M. Roussel. 2011. Performance characteristics of thin-lift overlay mixtures. Transportation Research Record: Journal of the Transportation Research Board, No. 2208, pp. 17–25.

15. Muhuanthan, B., Wu, Shenghua, Zhang, W., Shen, S., and Mohammad, L.2017. Case Study: Short-term Performance and Material Property Evolution of Warm Mix Asphalt and Hot Mix Asphalt Pavements. Transportation Research Record: Journal of the Transportation Research Board, Washington, D.C.

16. Ozer, H., I. L. Al-Qadi, and A. Kanaan. 2012. Laboratory Evaluation of High Asphalt Binder Replacement with Recycled Asphalt Shingles (RAS) for a Low N-Design Asphalt Mixture. Report No. FHWA-ICT-12-018. Illinois Center for Transportation, Rantoul, IL.

17. Swamy, K. A., Mitchell, L. F., Hall, S. J., & Sias Daniel, J. 2010. Impact of RAP on the volumetric, stiffness, strength, and low-temperature properties of HMA. Journal of Materials in Civil Engineering, 23(11), 1490-1497.

18. Tabaković, A., A. Gibney, C. McNally, and M. Gilchrist. 2010. Influence of recycled asphalt pavement on fatigue performance of asphalt concrete base courses. Journal of Materials in Civil Engineering, Vol. 22, No. 6, pp. 643–650.

19. Valdes, G., Perez, F., Miró, R., and Martinez, A. 2010. Experimental Study of Recycled Asphalt Mixtures with High Percentages of Reclaimed Asphalt Pavement (RAP). Proceedings of the Annual Meeting of the Transportation Research Board. Washington, D.C.

20. Vavrik, W. R., S. H. Carpenter, S. Gillen, J. Behnke, and F. Garrott. 2008. Evaluation of Field-Produced Hot Mix Asphalt (HMA) Mixtures with Fractionated Recycled Asphalt Pavement (RAP): 2008 Illinois Tollway Field Mix Trials. Report No. ICT-08-030. Illinois Center for Transportation, Rantoul, IL.

21. West, R., Willis, J.R., and Marasteanu, M. Improved mix design, evaluation, and materials management practices for hot mix asphalt with high reclaimed asphalt pavement content. Auburn, AL: National Center for Asphalt Technology, Report Number NCHRP 752, 2013.

22. Williams, R. C. 2010. Performance of Recycled Asphalt Shingles in Hot Mix Asphalt. Report No. TPS5(213), Pooled Fund Study. Institute for Transportation, Iowa State University, Ames, IA.

23. Williams, R. C., A. Cascione, D. S. Haugen, W. G. Buttlar, R. A. Bentsen, and J. Behnke. 2011. Characterization of Hot Mix Asphalt Containing Post-Consumer Recycled Asphalt Shingles and Fractionated Reclaimed Asphalt Pavement. Final Report Submitted to the Illinois State Toll Highway Authority. Iowa State University, Ames IA

24. Witczak, M. W., Kaloush, K., Pellinen, T., El-Basyouny, M., and Von Quintus, H. 2002. Simple Performance Test for Superpave Mix Design. NCHRP Report 465. Washington, DC.

25. Xiao, F., S. Amirkhanian, and C. H. Juang. 2007. Rutting resistance of rubberized asphalt concrete pavements containing reclaimed asphalt pavement mixtures. Journal of Materials in Civil Engineering, Vol. 19, No. 6, pp. 475–483.

26. Zhou, F., Hu, S., and Scullion, T. 2006. Integrated Asphalt (Overlay) Mixture Design Balancing Rutting and Cracking Requirements. FHWA/TX-06/0-5123-1. Texas Transportation Institute, College Station, Texas.

27. Zhou, F., S. Hu, and T. Scullion. 2013. Balanced RAP/RAS Mix Design and Performance Evaluation System for Project-Specific Service Conditions, Research Report FHWA/TX-13/0-6092-3, Texas A&M Transportation Institute, College Station, Texas.

Appendix A: Evaluation of Pavement Materials

Table A1 Aggregate Gradation with Percent Materials Passing for RAP Source A

Sieve Size	Percent Passing				
	Master Mix	RAP	15% RAP Blend	30% RAP Blend	45% RAP Blend
3/4"	**100.0**	100.0	100.0	100.0	100.0
1/2"	**94.2**	98.9	93.4	92.2	90.3
3/8"	**81.0**	92.0	79.1	76.3	72.0
#4	**52.0**	71.6	48.6	43.3	36.0
#8	**37.5**	53.8	34.7	30.5	24.2
#16	**25.5**	42.8	22.5	18.1	11.4
#30	**16.4**	34.9	13.2	8.5	1.2
#50	**12.0**	24.4	9.9	6.7	1.2
#200	**5.0**	9.3	4.2	3.2	1.2

Table A2 Aggregate Gradation with Percent Materials Passing for RAP source B

Sieve Size	Percent Passing				
	Master Mix	RAP	15% RAP Blend	30% RAP Blend	45% RAP Blend
3/4"	**100.0**	100.0	100.0	100.0	100.0
1/2"	**94.2**	100.0	93.2	91.7	89.4
3/8"	**81.0**	92.2	79.0	76.2	71.8
#4	**52.0**	65.6	49.6	46.1	40.9
#8	**37.5**	47.0	35.8	33.4	29.8
#16	**25.5**	39.2	23.1	19.6	14.3
#30	**16.4**	29.5	14.1	10.8	5.7
#50	**12.0**	22.9	10.1	7.3	3.0
#200	**5.0**	11.9	3.8	2.1	0

Table A3 Ignition Oven for RAP to Obtain Asphalt Content

Sample #1

RAP Source A	
Total RAP	999,8
Asphalt Content:	5,6%

Sample #2

RAP Source A	
Total RAP	1001,3
Asphalt Content:	5,5%

Sample #3

RAP Source A	
Total RAP	1000,6
Asphalt Content:	5,5%

Sample #4

RAP Source A	
Total RAP	1000,5
Asphalt Content:	5,6%

Sample #1

RAP Source B	
Total RAP	1199,5
Asphalt Content:	5,3%

Sample #2

RAP Source B	
Total RAP	1198,7
Asphalt Content:	5,3%

Sample #3

RAP Source B	
Total RAP	1202,0
Asphalt Content:	5,3%

Sample #4

RAP Source B	
Total RAP	1202,1
Asphalt Content:	5,5%

Appendix B: Performance Test Analysis

Table B1 IDT Results: Asphalt Binder PG (Dolomite PG 64-22)

Specimen	Air Voids, %	Max Load, lbs	Displacement at Maximum Load, in.	Tensile Strength, psi
1	6.7	1515	0.11	64
2	7.0	1461	0.12	62
3	6.9	1620	0.13	69
4	7.5	1481	0.12	63
Average	7.0	1519	0.12	64
Std Dev	0.3	61	0.01	3
COV	4%	4%	6%	4%

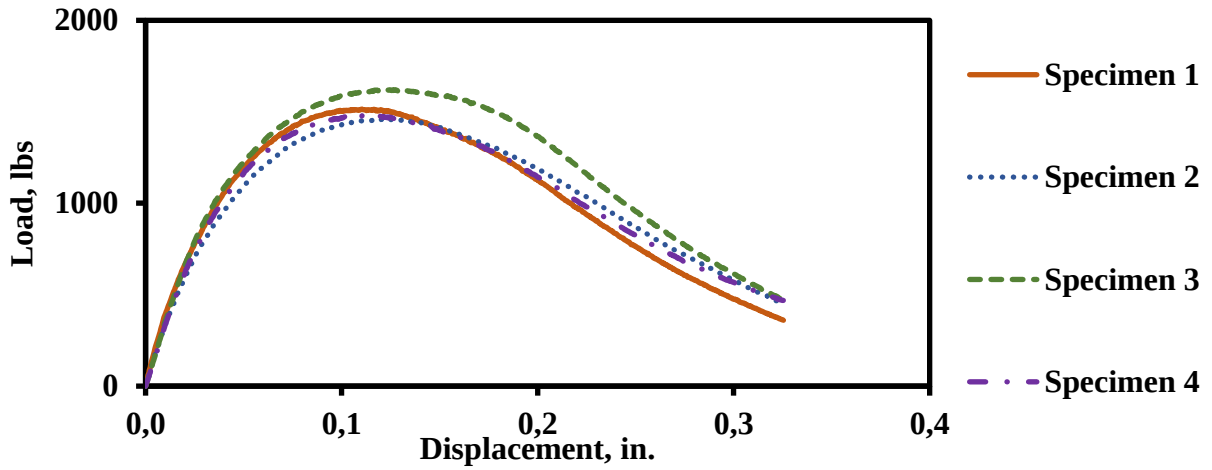

Figure B2 IDT results: Asphalt Binder PG (Dolomite PG 64-22)

Table B2 OT Results: Asphalt Binder PG (Dolomite PG 64-22)

Specimen	Air Voids, %	Max Load, lbs	Work of Fracture, in.-lbs	Critical Fracture Energy, in.-lbs/in.²	Crack Progression Rate	Number of Cycles
1	7.2	444.3	5.0	1.1	0.4	857
2	7.5	354.0	4.3	0.9	0.4	1000
3	7.7	346.6	5.2	1.2	0.4	904
4	7.2	334.3	4.5	1.0	0.3	1000
Average	7.4	369.8	4.7	1.0	0.4	940
Std Dev	0.2	43.6	0.4	0.1	0.0	62
COV	3%	12%	8%	8%	3%	7%

Table B3 IDT Results: Asphalt Binder PG (Dolomite PG 70-22)

Specimen	Air Voids, %	Max Load, lbs	Displacement at Maximum Load, in.	Tensile Strength, psi
1	7.2	2414	0.10	102
2	6.9	2559	0.11	109
3	6.9	2336	0.12	99
4	6.9	2152	0.14	91
Average	7.0	2366	0.12	100
Std Dev	0.1	147	0.01	6
COV	2%	6%	11%	6%

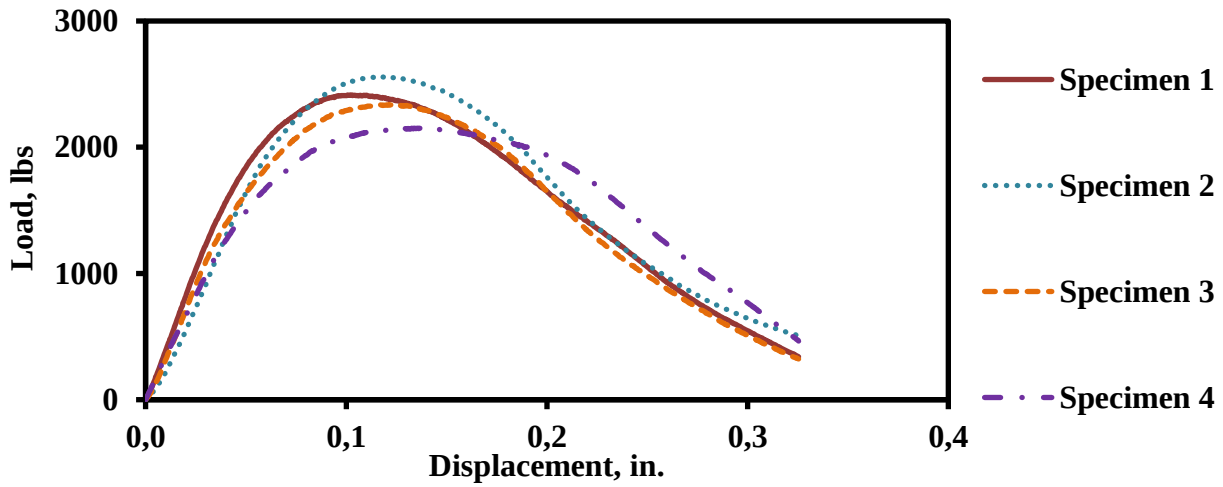

Figure B2 IDT results: Asphalt Binder PG (Dolomite PG 70-22)

Table B4 OT Results: Asphalt Binder PG (Dolomite PG 70-22)

Specimen	Air Voids, %	Max Load, lbs	Work of Fracture, in.-lbs	Critical Fracture Energy, in.-lbs/in.²	Crack Progression Rate	Number of Cycles to Failure
1	7.4	564.2	10.8	2.4	0.3	1000
2	7.3	514.8	9.6	2.1	0.3	1000
3	7.0	525.4	10.8	2.4	0.3	1000
Average	7.2	534.8	10.4	2.3	0.3	1000
Std Dev	0.2	21.2	0.6	0.1	0.0	0
COV	0.0	4%	6%	6%	2%	0%

Table B5 IDT Results: Asphalt Binder PG (Dolomite PG 76-22)

Specimen	Air Voids, %	Max Load, lbs	Displacement at Maximum Load, in.	Tensile Strength, psi
1	8.0	2815	0.13	119
2	7.8	2825	0.12	120
3	7.8	2678	0.13	114
4	7.6	2889	0.11	123
Average	7.8	2802	0.12	119
Std Dev	0.1	77	0.01	3
COV	2%	3%	7%	3%

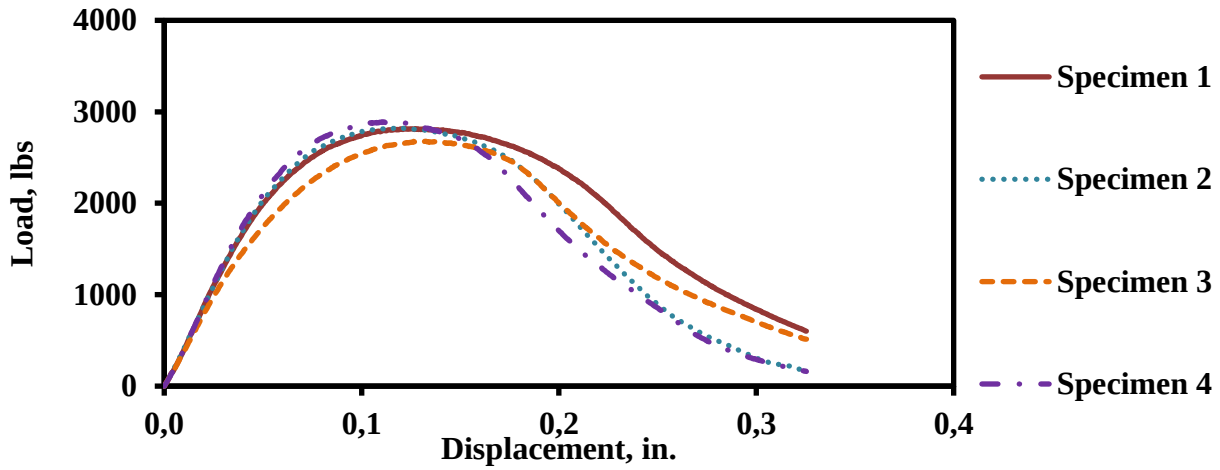

Figure B3 IDT results: Asphalt Binder PG (Dolomite PG 76-22)

Table B6 OT Results: Asphalt Binder PG (Dolomite PG 76-22)

Specimen	Air Voids, %	Max Load, lbs	Work of Fracture, in.-lbs	Critical Fracture Energy, in.-lbs/in.²	Crack Progression Rate	Number of Cycles to Failure
1	8	653.4	12.0	2.7	0.3	865
2	7.7	777.4	13.0	2.9	0.4	337
3	7.6	845.4	11.9	2.7	0.3	1000
Average	7.8	758.7	12.3	2.7	0.3	734
Std Dev	0.2	79.5	0.5	0.1	0.0	286
COV	2%	10%	4%	4%	8%	39%

Table B7 IDT Results: Asphalt Binder PG (Granite PG 64-22)

Specimen	Air Voids, %	Max Load, lbs	Displacement at Maximum Load, in.	Tensile Strength, psi
1	7.1	1951	0.13	83
2	7.2	1801	0.14	76
4	7.2	1827	0.15	78
Average	7.2	1860	0.14	79
Std Dev	0.0	66	0.01	3
COV	1%	4%	7%	4%

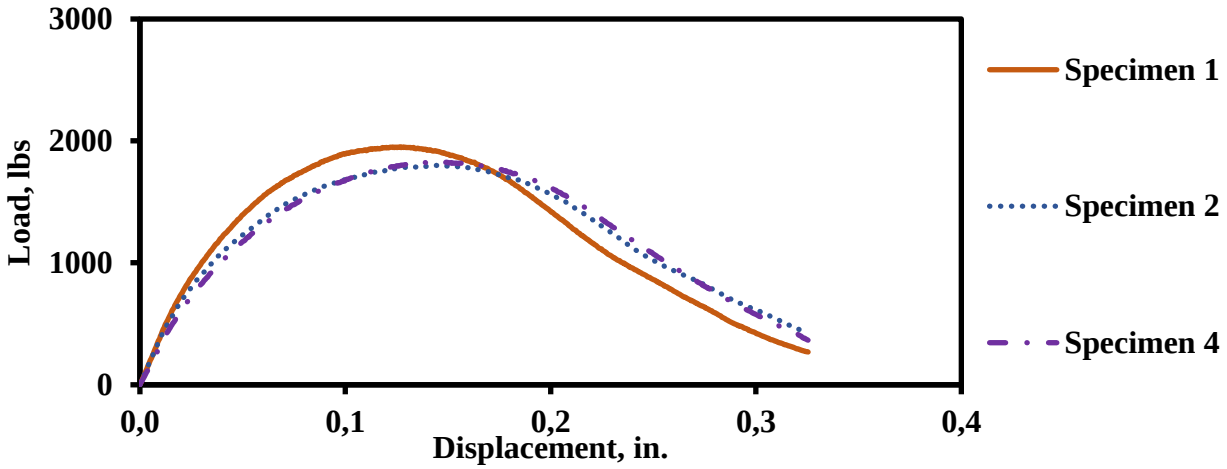

Figure B4Granite IDT results: Asphalt Binder PG (Granite PG 64-22)

Table B8 OT Results: Asphalt Binder PG (Granite PG 64-22)

Specimen	Air Voids, %	Max Load, lbs	Work of Fracture, in.-lbs	Critical Fracture Energy, in.-lbs/in.²	Crack Progression Rate	Number of Cycles to Failure
1	7.5	418.8	7.2	1.6	0.3	1000
2	7.3	338.9	6.7	1.5	0.3	1000
3	7.5	376.2	7.7	1.7	0.3	1000
4	6.9	376.2	5.7	1.3	0.3	1000
Average	7.3	377.5	6.8	1.5	0.3	1000
Std Dev	0.2	28.3	0.8	0.2	0.0	0
COV	3%	7%	11%	11%	6%	0%

Table B9 IDT Results: Asphalt Binder PG (Granite PG 70-22)

Specimen	Air Voids, %	Max Load, lbs	Displacement at Maximum Load, in.	Tensile Strength, psi
2	7.4	2312	0.15	98
3	7.4	2129	0.16	90
4	7.0	2235	0.15	95
Average	7.3	2225	0.15	94
Std Dev	0.2	75	0.00	3
COV	3%	3%	2%	3%

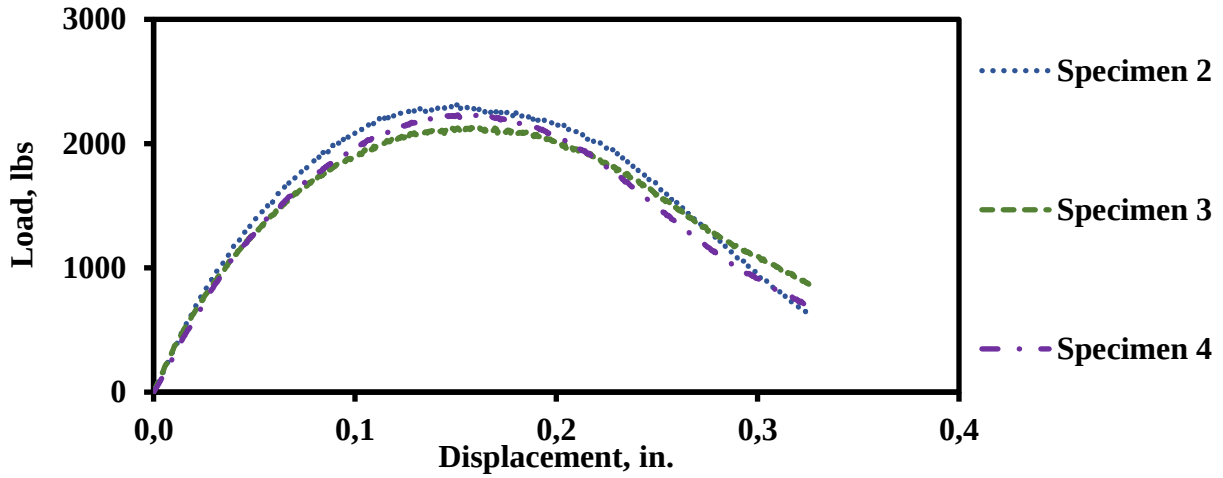

Figure B5Granite IDT results: Asphalt Binder PG (Granite PG 70-22)

Table B10 OT Results: Asphalt Binder PG (Granite PG 70-22)

Specimen	Air Voids, %	Max Load, lbs	Work of Fracture, in.-lbs	Critical Fracture Energy, in.-lbs/in.²	Crack Progression Rate	Number of Cycles to Failure
2	7.8	446.8	8.8	2.0	0.3	1000
3	8.0	414.9	8.5	1.9	0.3	1000
4	7.8	428.2	8.9	2.0	0.3	1000
Average	7.9	430.0	8.7	1.9	0.3	1000
Std Dev	0.1	13.1	0.2	0.0	0.0	0
COV	1%	3%	2%	2%	2%	0%

Table B11 IDT Results: Asphalt Binder PG (Granite PG 76-22)

Specimen	Air Voids, %	Max Load, lbs	Displacement at Maximum Load, in.	Tensile Strength, psi
2	7.5	3205	0.13	136
3	7.2	3020	0.14	128
4	6.9	2790	0.14	118
Average	7.2	3005	0.14	128
Std Dev	0.2	170	0.01	7
COV	3%	6%	6%	6%

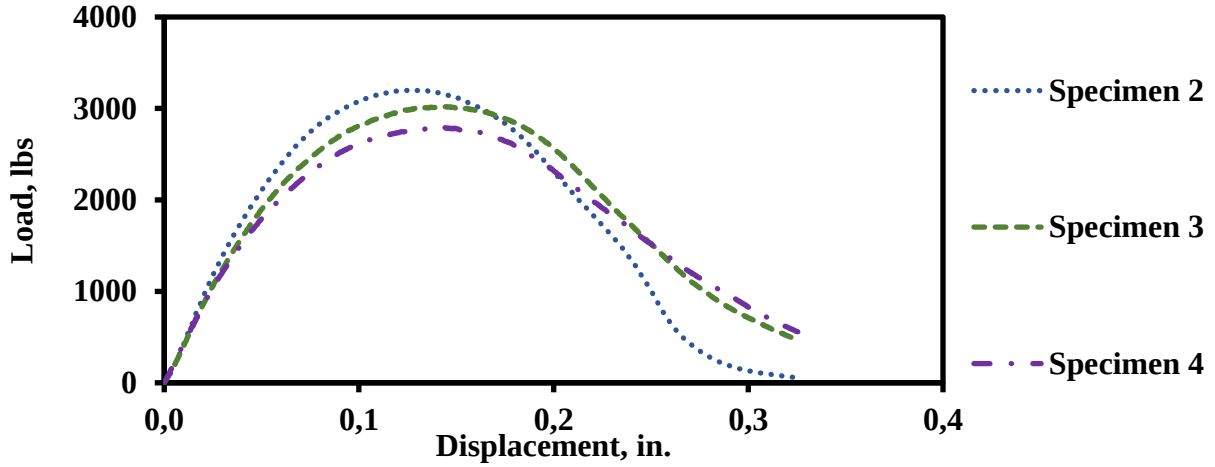

Figure B6Granite IDT results: Asphalt Binder PG (Granite PG 76-22)

Table B12 OT Results: Asphalt Binder PG (Granite PG 76-22)

Specimen	Air Voids, %	Max Load, lbs	Work of Fracture, in.-lbs	Critical Fracture Energy, in.-lbs/in.²	Crack Progression Rate	Number of Cycles to Failure
1	7.5	568.1	11.1	2.5	0.2	1000
2	7.8	572.2	11.3	2.5	0.3	1000
3	7.7	522.8	10.6	2.4	0.2	1000
4	7.5	473.5	8.7	1.9	0.2	1000
Average	7.6	534.1	10.4	2.3	0.2	1000
Std Dev	0.1	40.0	1.0	0.2	0.0	0
COV	2%	7%	10%	10%	7%	0%

Table B13 IDT Results: Asphalt Binder Source (PG 64-22 Source A)

Specimen	Air Voids, %	Max Load, lbs	Displacement at Maximum Load, in.	Tensile Strength, psi
1	6.7	1515	0.11	64
2	7.0	1461	0.12	62
3	6.9	1620	0.13	69
4	7.5	1481	0.12	63
Average	7.0	1519	0.12	64
Std Dev	0.3	61	0.01	3
COV	4%	4%	6%	4%

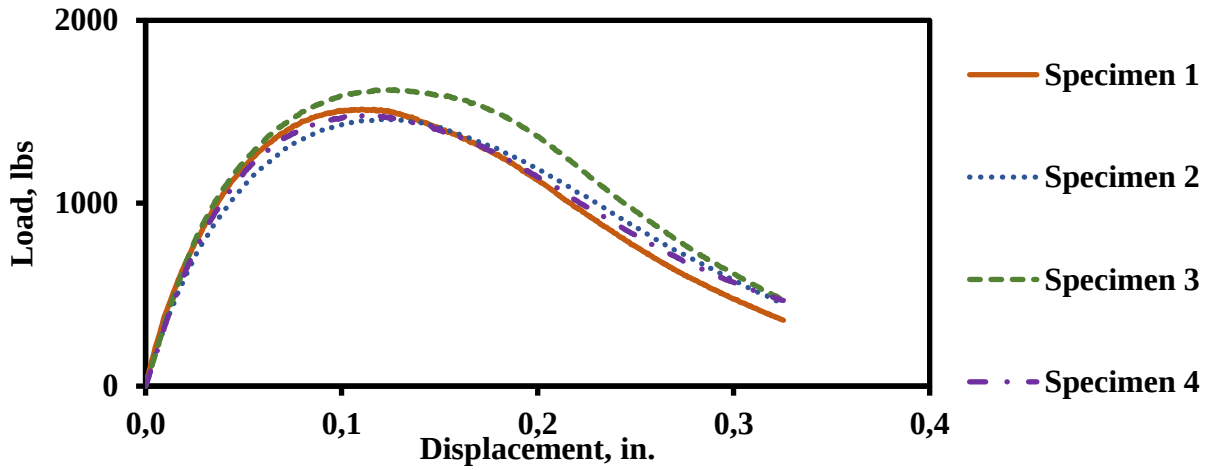

Figure B7 IDT results: Asphalt Binder Source (PG 64-22 Source A)

Table B14 OT Results: Asphalt Binder Source (PG 64-22 Source A)

Specimen	Air Voids, %	Max Load, lbs	Work of Fracture, in.-lbs	Critical Fracture Energy, in.-lbs/in.²	Crack Progression Rate	Number of Cycles
1	7.2	444.3	5.0	1.1	0.4	857
2	7.5	354.0	4.3	0.9	0.4	1000
3	7.7	346.6	5.2	1.2	0.4	904
4	7.2	334.3	4.5	1.0	0.3	1000
Average	7.4	369.8	4.7	1.0	0.4	940
Std Dev	0.2	43.6	0.4	0.1	0.0	62
COV	3%	12%	8%	8%	3%	7%

Table B15 IDT Results: Asphalt Binder Source (PG 64-22 Source B)

Specimen	Air Voids, %	Max Load, lbs	Displacement at Maximum Load, in.	Tensile Strength, psi
1	7.0	1316	0.13	56
2	6.7	1384	0.13	59
3	6.8	1377	0.13	58
4	6.4	1238	0.14	53
Average	6.7	1329	0.13	56
Std Dev	0.2	59	0.00	2
COV	3%	4%	3%	4%

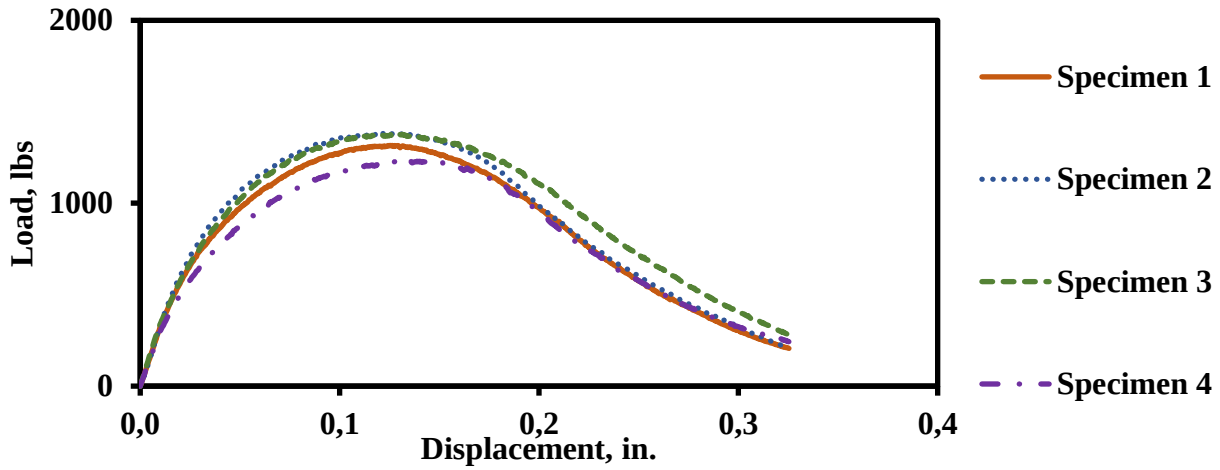

Figure B8 IDT results: Asphalt Binder Source (PG 64-22 Source B)

Table B16 OT Results: Asphalt Binder Source (PG 64-22 Source B)

Specimen	Air Voids, %	Max Load, lbs	Work of Fracture, in.-lbs	Critical Fracture Energy, in.-lbs/in.²	Crack Progression Rate	Number of Cycles to Failure
1	7.0	245.5	4.1	0.9	0.2	1000
2	6.7	318.8	6.3	1.4	0.3	1000
3	6.8	274.8	4.8	1.1	0.3	1000
4	6.4	258.8	4.1	0.9	0.3	1000
Average	6.7	274.5	4.8	1.1	0.3	1000
Std Dev	0.2	27.6	0.9	0.2	0.0	0
COV	3%	10%	18%	18%	5%	0%

Table B17 IDT Results: Asphalt Binder Source (PG 64-22 Source C)

Specimen	Air Voids, %	Max Load, lbs	Displacement at Maximum Load, in.	Tensile Strength, psi
1	8.0	1555	0.14	66
2	7.2	1460	0.13	62
3	7.8	1388	0.11	59
4	7.0	1567	0.12	67
Average	7.5	1493	0.12	63
Std Dev	0.4	73	0.01	3
COV	5%	5%	8%	5%

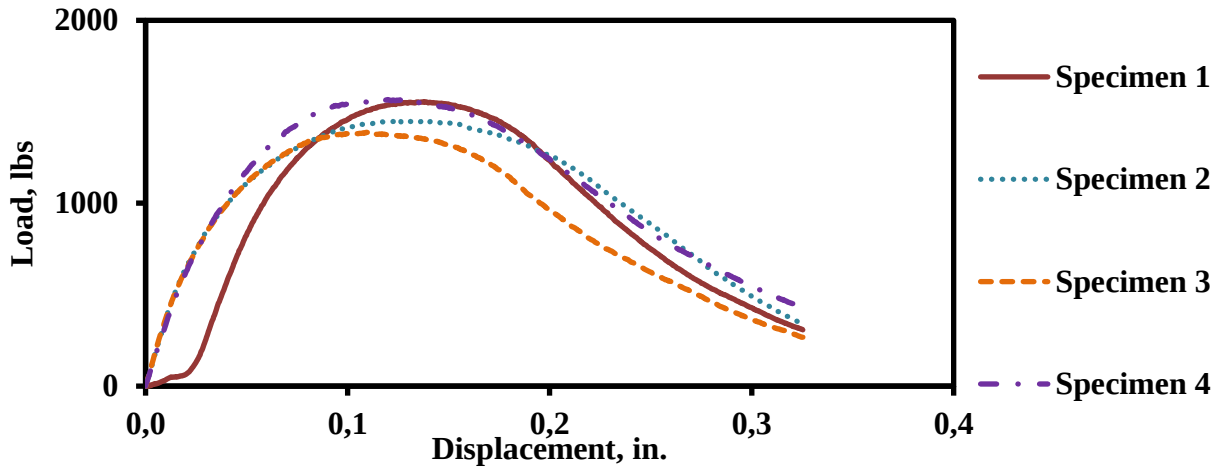

Figure B9 IDT results: Asphalt Binder Source (PG 64-22 Source C)

Table B18 OT Results: Asphalt Binder Source (PG 64-22 Source C)

Specimen	Air Voids, %	Max Load, lbs	Work of Fracture, in.-lbs	Critical Fracture Energy, in.-lbs/in.²	Crack Progression Rate	Number of Cycles to Failure
1	7.4	357.5	4.5	1.0	0.3	1000
2	8.0	401.5	5.3	1.2	0.3	1000
Average	7.7	379.5	4.9	1.1	0.3	1000
Std Dev	0.3	22.0	0.4	0.1	0.0	0
COV	4%	6%	8%	8%	5%	0%

Table B19 IDT Results: Asphalt Binder Source (PG 64-22 Source D)

Specimen	Air Voids, %	Max Load, lbs	Displacement at Maximum Load, in.	Tensile Strength, psi
1	7.2	1757	0.13	75
2	7.1	1729	0.15	73
3	7.5	1772	0.14	75
4	7.1	1674	0.12	71
Average	7.2	1733	0.14	74
Std Dev	0.2	38	0.01	2
COV	2%	2%	7%	2%

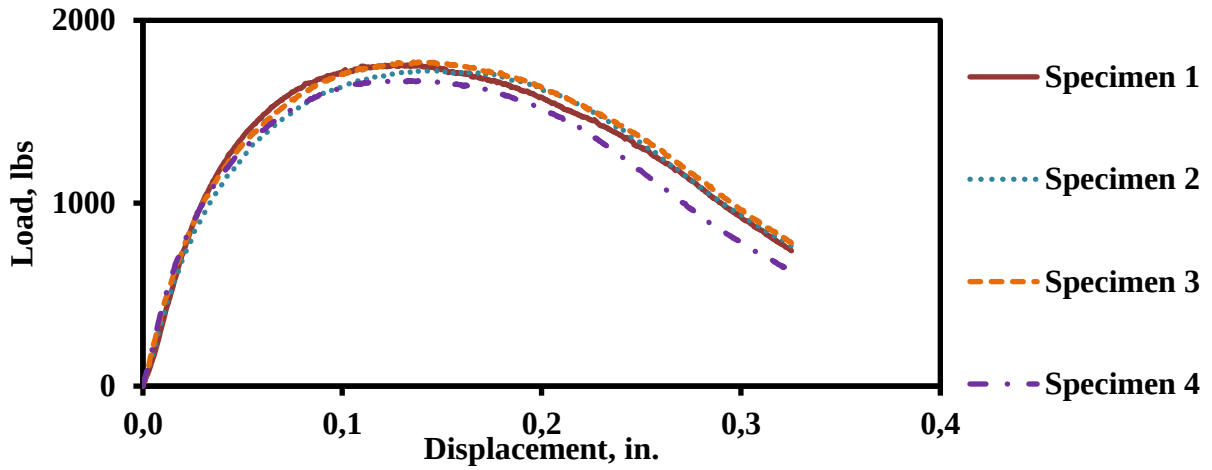

Figure B10 IDT results: Asphalt Binder Source (PG 64-22 Source D)

Table B20 OT Results: Asphalt Binder Source (PG 64-22 Source D)

Specimen	Air Voids, %	Max Load, lbs	Work of Fracture, in.-lbs	Critical Fracture Energy, in.-lbs/in.²	Crack Progression Rate	Number of Cycles to Failure
1	7.9	369.5	4.5	1.0	0.3	1000
2	7.6	348.2	6.5	1.5	0.3	1000
3	8.0	224.3	3.9	0.9	0.3	1000
4	8.0	304.2	4.8	1.1	0.3	1000
Average	7.9	311.5	4.9	1.1	0.3	1000
Std Dev	0.2	55.6	1.0	0.2	0.0	0
COV	2%	18%	20%	20%	2%	0%

Table B21 IDT Results: Asphalt Binder Source (PG 64-22 Source E)

Specimen	Air Voids, %	Max Load, lbs	Displacement at Maximum Load, in.	Tensile Strength, psi
1	6.7	1572	0.12	67
2	6.7	1689	0.12	72
3	7.0	1540	0.14	65
4	6.5	1697	0.13	72
Average	6.7	1625	0.13	69
Std Dev	0.2	70	0.01	3
COV	3%	4%	9%	4%

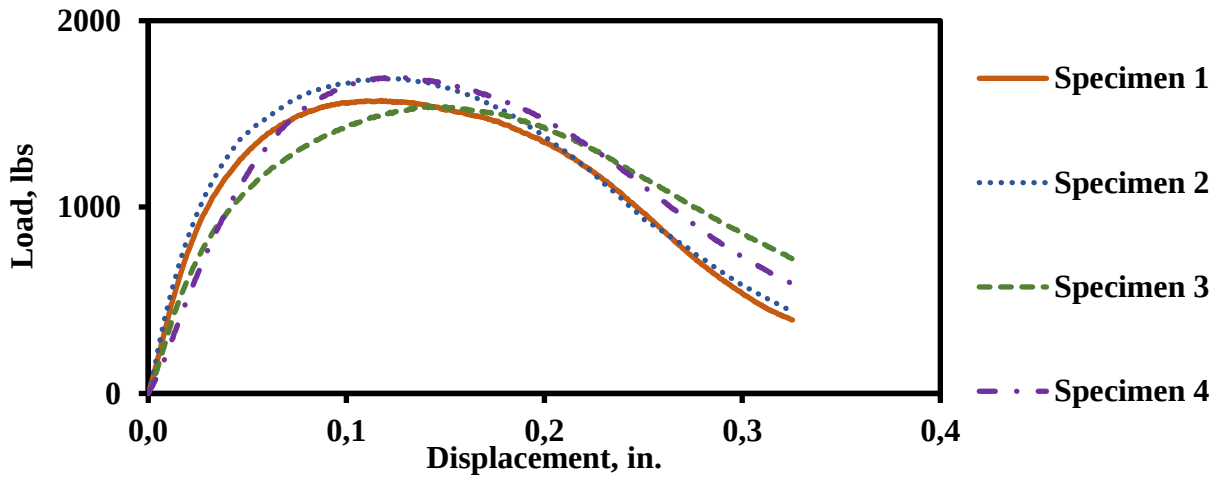

Figure B11 IDT results: Asphalt Binder Source (PG 64-22 Source E)

Table B22 OT Results: Asphalt Binder Source (PG 64-22 Source E)

Specimen	Air Voids, %	Max Load, lbs	Work of Fracture, in.-lbs	Critical Fracture Energy, in.-lbs/in.²	Crack Progression Rate	Number of Cycles to Failure
1	6.7	337.6	5.7	1.3	0.3	1000
2	7.4	336.1	5.7	1.3	0.3	1000
3	6.7	349.5	6.3	1.4	0.3	1000
Average	6.9	341.1	5.9	1.3	0.3	1000
Std Dev	0.3	6.0	0.3	0.1	0.0	0
COV	5%	2%	5%	5%	4%	0%

Table B23 IDT Results: Asphalt Binder Source (PG 70-22 Source A)

Specimen	Air Voids, %	Max Load, lbs	Displacement at Maximum Load, in.	Tensile Strength, psi
1	7.2	2414	0.10	102
2	6.9	2559	0.11	109
3	6.9	2336	0.12	99
4	6.9	2152	0.14	91
Average	7.0	2366	0.12	100
Std Dev	0.1	147	0.01	6
COV	2%	6%	11%	6%

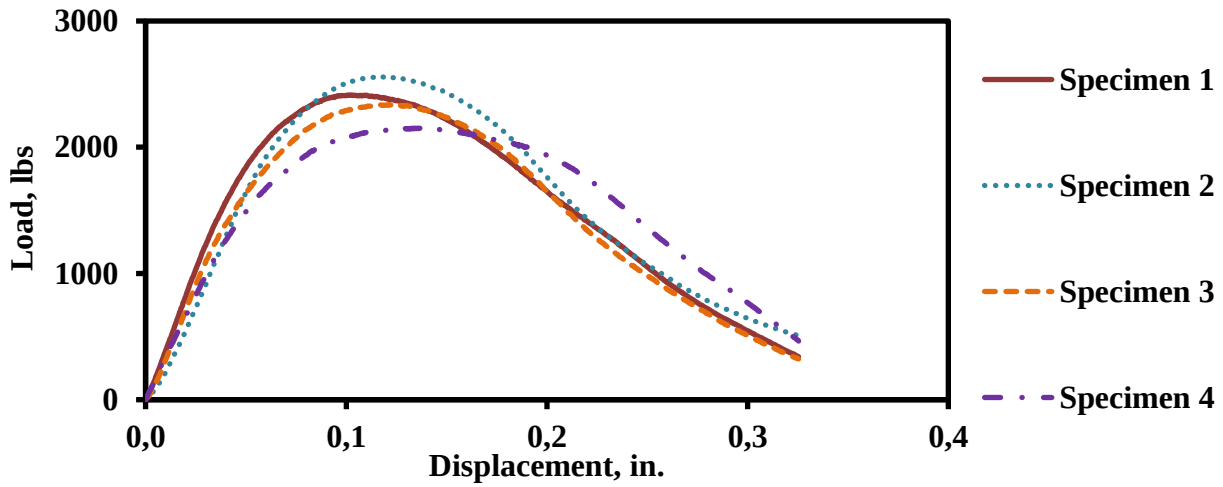

Figure B12 IDT results: Asphalt Binder Source (PG 70-22 Source A)

Table B24 OT Results: Asphalt Binder Source (PG 70-22 Source A)

Specimen	Air Voids, %	Max Load, lbs	Work of Fracture, in.-lbs	Critical Fracture Energy, in.-lbs/in.²	Crack Progression Rate	Number of Cycles to Failure
1	7.4	564.2	10.8	2.4	0.3	1000
2	7.3	514.8	9.6	2.1	0.3	1000
3	7.0	525.4	10.8	2.4	0.3	1000
Average	7.2	534.8	10.4	2.3	0.3	1000
Std Dev	0.2	21.2	0.6	0.1	0.0	0
COV	0.0	4%	6%	6%	2%	0%

Table B25 IDT Results: Asphalt Binder Source (PG 70-22 Source B)

Specimen	Air Voids, %	Max Load, lbs	Displacement at Maximum Load, in.	Tensile Strength, psi
1	7.0	1077	0.10	46
2	6.8	1006	0.11	43
3	6.8	1004	0.10	43
4	6.3	928	0.10	39
Average	6.7	1004	0.10	43
Std Dev	0.3	53	0.01	2
COV	4%	5%	5%	5%

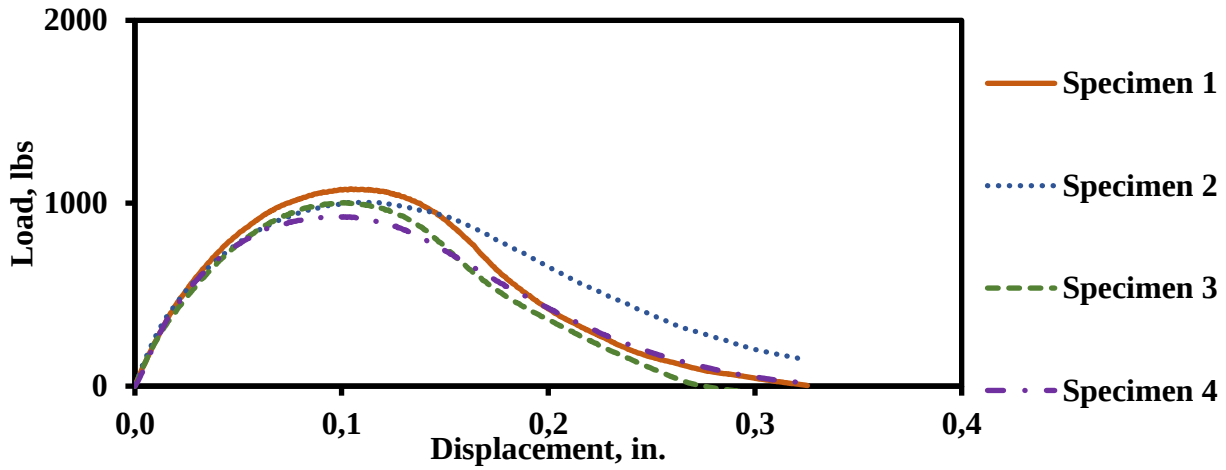

Figure B13 IDT results: Asphalt Binder Source (PG 70-22 Source B)

Table B26 OT Results: Asphalt Binder Source (PG 70-22 Source B)

Specimen	Air Voids, %	Max Load, lbs	Work of Fracture, in.-lbs	Critical Fracture Energy, in.-lbs/in.²	Crack Progression Rate	Number of Cycles to Failure
1	7.5	210.9	2.3	0.5	0.3	1000
2	7.1	234.9	2.7	0.6	0.4	330
3	7.1	224.3	2.4	0.5	0.3	1000
4	7.2	189.6	3.0	0.7	0.3	1000
Average	7.2	214.9	2.6	0.6	0.3	833
Std Dev	0.2	16.9	0.3	0.1	0.1	290
COV	2%	8%	10%	10%	16%	35%

Table B27 IDT Results: Asphalt Binder Source (PG 70-22 Source C)

Specimen	Air Voids, %	Max Load, lbs	Displacement at Maximum Load, in.	Tensile Strength, psi
1	7.4	2061	0.13	87
2	7.5	2001	0.14	85
3	7.0	2080	0.15	88
4	6.8	2069	0.14	88
Average	7.2	2053	0.14	87
Std Dev	0.3	31	0.00	1
COV	4%	1%	3%	1%

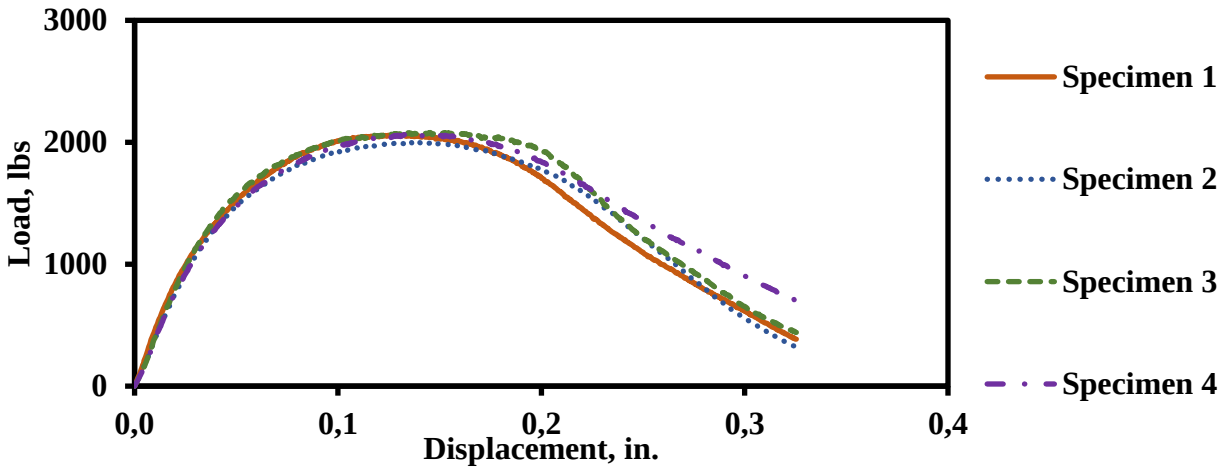

Figure B14 IDT results: Asphalt Binder Source (PG 70-22 Source C)

Table B28 OT Results: Asphalt Binder Source (PG 70-22 Source C)

Specimen	Air Voids, %	Max Load, lbs	Work of Fracture, in.-lbs	Critical Fracture Energy, in.-lbs/in.²	Crack Progression Rate	Number of Cycles to Failure
1	7.4	528.2	7.0	1.5	0.3	1000.0
2	8.0	428.2	6.8	1.5	0.3	1000.0
3	7.9	450.9	6.9	1.5	0.3	1000.0
4	7.9	501.4	7.7	1.7	0.3	1000.0
Average	7.8	477.2	7.1	1.6	0.3	1000.0
Std Dev	0.2	39.6	0.4	0.1	0.0	0.0
COV	3%	8%	5%	5%	4%	0%

Table B29 IDT Results: Asphalt Binder Source (PG 70-22 Source D)

Specimen	Air Voids, %	Max Load, lbs	Displacement at Maximum Load, in.	Tensile Strength, psi
1	7.7	2827	0.17	120
2	7.9	2665	0.15	113
3	7.9	2424	0.18	103
4	7.7	2677	0.16	114
Average	7.8	2648	0.17	112
Std Dev	0.1	145	0.01	6
COV	1%	5%	7%	5%

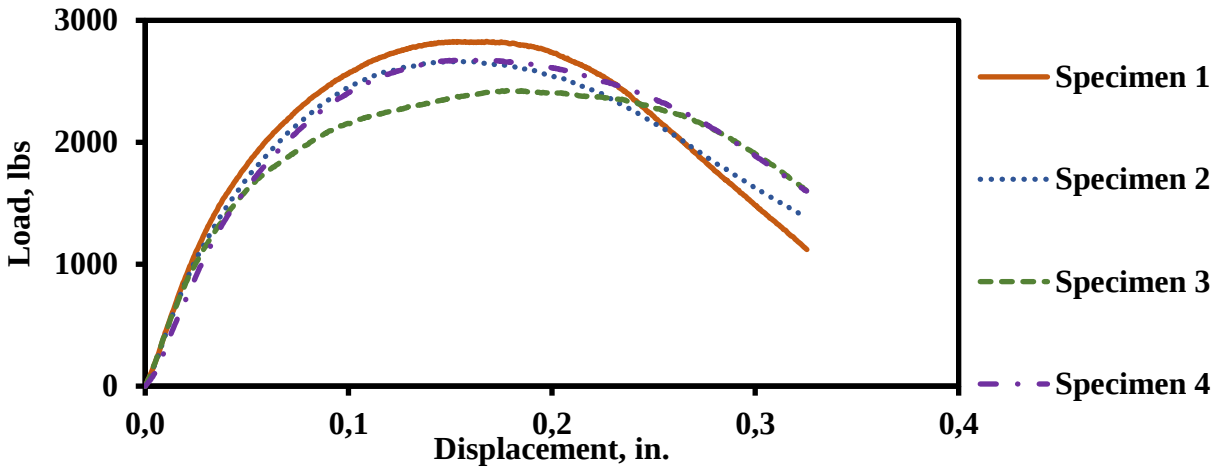

Figure B15 IDT results: Asphalt Binder Source (PG 70-22 Source D)

Table B30 OT Results: Asphalt Binder Source (PG 70-22 Source D)

Specimen	Air Voids, %	Max Load, lbs	Work of Fracture, in.-lbs	Critical Fracture Energy, in.-lbs/in.²	Crack Progression Rate	Number of Cycles to Failure
1	7.9	624.0	12.2	2.7	0.3	1000.0
2	7.9	676.0	13.4	3.0	0.3	1000.0
3	7.7	586.8	10.8	2.4	0.3	1000.0
4	7.7	610.8	11.6	2.6	0.3	1000.0
Average	7.8	624.4	12.0	2.7	0.3	1000.0
Std Dev	0.1	32.6	0.9	0.2	0.0	0.0
COV	1%	5%	8%	8%	6%	0%

Table B31 IDT Results: Asphalt Binder Source (PG 70-22 Source E)

Specimen	Air Voids, %	Max Load, lbs	Displacement at Maximum Load, in.	Tensile Strength, psi
1	7.5	1796	0.16	76
2	6.8	2091	0.13	89
3	7.2	1809	0.14	77
4	7.4	1882	0.14	80
Average	7.2	1895	0.14	80
Std Dev	0.3	118	0.01	5
COV	4%	6%	8%	6%

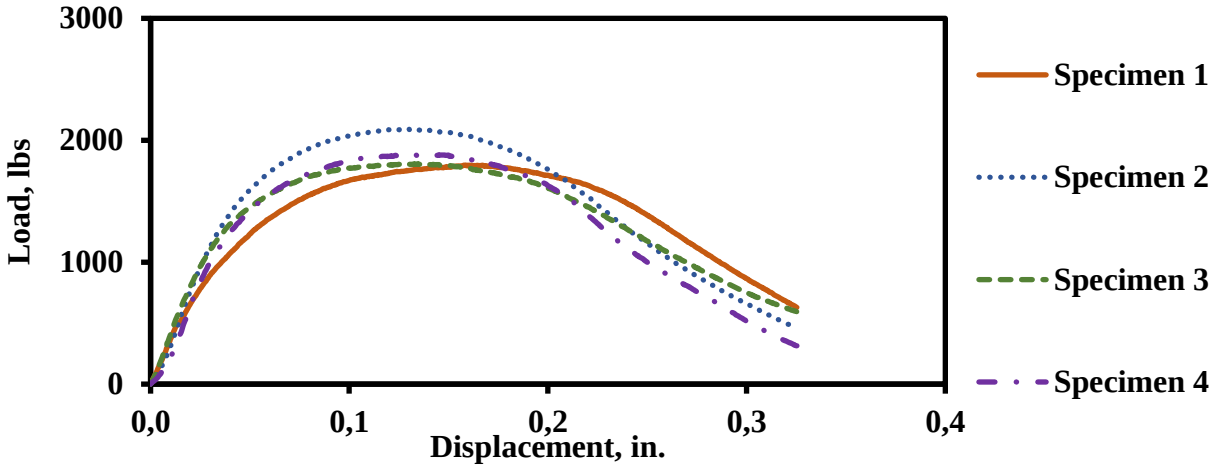

Figure B16 IDT results: Asphalt Binder Source (PG 70-22 Source E)

Table B32 OT Results: Asphalt Binder Source (PG 70-22 Source E)

Specimen	Air Voids, %	Max Load, lbs	Work of Fracture, in.-lbs	Critical Fracture Energy, in.-lbs/in.²	Crack Progression Rate	Number of Cycles to Failure
1	7.1	336.1	5.1	1.1	0.3	1000
2	7.0	446.8	5.2	1.2	0.3	1000
3	7.7	350.8	5.0	1.1	0.3	1000
Average	7.3	377.9	5.1	1.1	0.3	1000
Std Dev	0.3	49.1	0.1	0.0	0.0	0
COV	4%	13%	2%	2%	4%	0%

Table B33 IDT Results: RAP Content (Dolomite 15% RAP)

Specimen	Air Voids, %	Max Load, lbs	Displacement at Maximum Load, in.	Tensile Strength, psi
1	6.5	2096	0.11	89
2	6.7	2260	0.12	96
3	6.2	2116	0.11	90
4	7.1	2132	0.11	90
Average	6.6	2151	0.11	91
Std Dev	0.3	64	0.00	3
COV	5%	3%	4%	3%

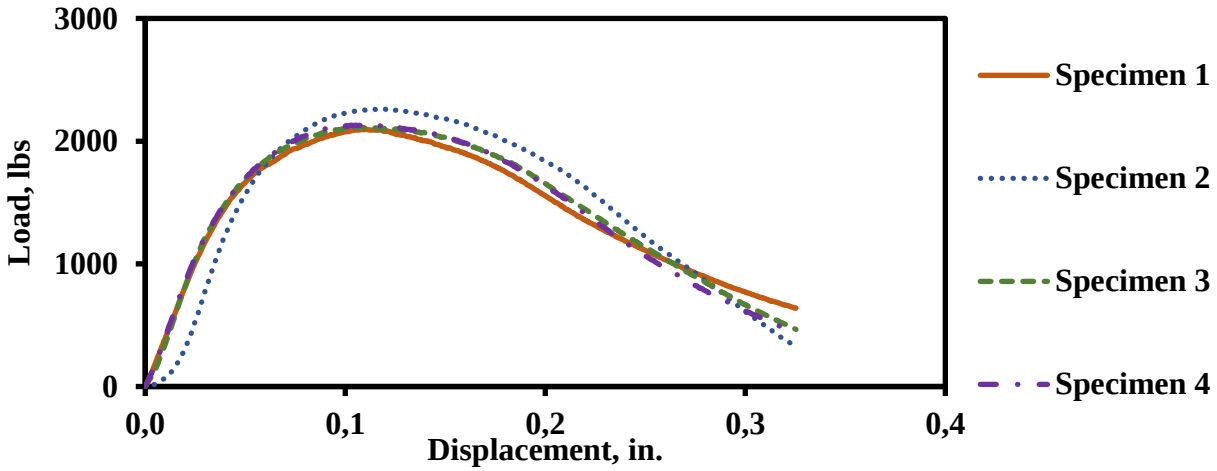

Figure B17 IDT results: RAP Content (Dolomite 15% RAP)

Table B34 OT Results: RAP Content (Dolomite 15% RAP)

Specimen	Air Voids, %	Max Load, lbs	Work of Fracture, in.-lbs	Critical Fracture Energy, in.-lbs/in.²	Crack Progression Rate	Number of Cycles to Failure
1	7.9	469.5	5.9	1.3	0.3	908
2	7.9	618.8	8.2	1.8	0.3	1000
4	8.0	493.4	5.8	1.3	0.3	1000
Average	7.9	527.2	6.6	1.5	0.3	969
Std Dev	0.0	65.5	1.1	0.3	0.0	43
COV	1%	12%	17%	17%	4%	4%

Table B35 IDT Results: RAP Content (Dolomite 30% RAP)

Specimen	Air Voids, %	Max Load, lbs	Displacement at Maximum Load, in.	Tensile Strength, psi
1	7.2	2806	0.11	119
2	6.7	3013	0.10	128
3	6.5	2889	0.10	123
4	6.3	2875	0.09	122
Average	6.7	2896	0.10	123
Std Dev	0.3	75	0.01	3
COV	5%	3%	7%	3%

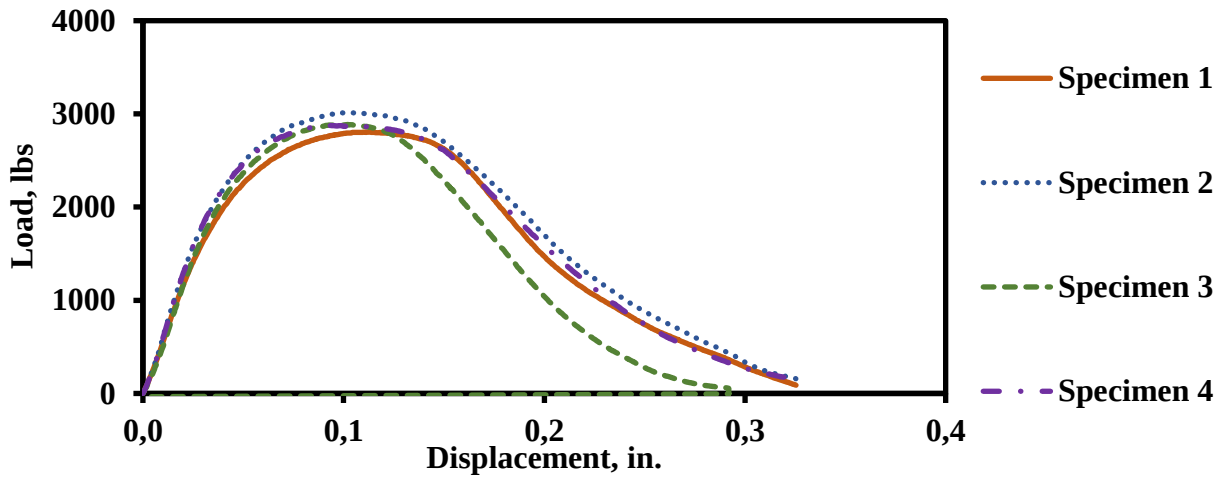

Figure B18 IDT results: RAP Content (Dolomite 30% RAP)

Table B36 OT Results: RAP Content (Dolomite 30% RAP)

Specimen	Air Voids, %	Max Load, lbs	Work of Fracture, in.-lbs	Critical Fracture Energy, in.-lbs/in.²	Crack Progression Rate	Number of Cycles to Failure
1	6.7	761.4	9.7	2.2	0.4	549
3	6.8	898.7	11.3	2.5	0.4	252
4	7.0	874.7	11.7	2.6	0.4	172
Average	6.8	845.0	10.9	2.4	0.4	324
Std Dev	0.1	59.9	0.9	0.2	0.0	162
COV	2%	7%	8%	8%	7%	50%

Table B37 IDT Results: RAP Content (Dolomite 45% RAP)

Specimen	Air Voids, %	Max Load, lbs	Displacement at Maximum Load, in.	Tensile Strength, psi
1	6.9	2335	0.12	99
2	6.4	2228	0.11	95
3	6.7	2420	0.12	103
4	6.5	2261	0.12	96
Average	6.6	2311	0.12	98
Std Dev	0.2	74	0.00	3
COV	3%	3%	2%	3%

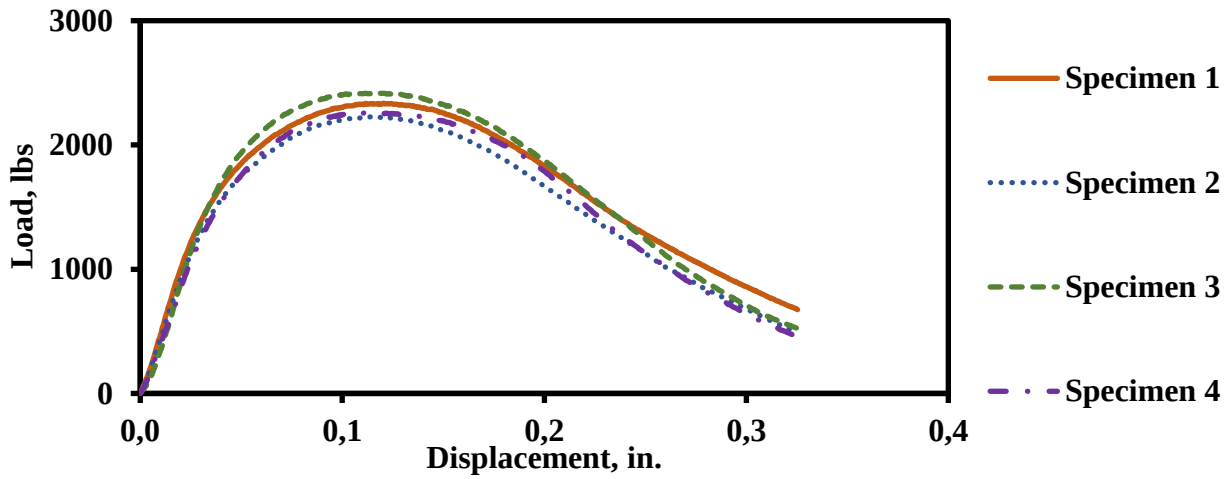

Figure B19 IDT results: RAP Content (Dolomite 45% RAP)

Table B38 OT Results: RAP Content (Dolomite 45% RAP)

Specimen	Air Voids, %	Max Load, lbs	Work of Fracture, in.-lbs	Critical Fracture Energy, in.-lbs/in.²	Crack Progression Rate	Number of Cycles to Failure
1	6.9	732.1	11.0	2.5	0.3	1000
2	7.4	756.1	11.0	2.4	0.4	458
Average	7.2	744.1	11.0	2.4	0.3	729
Std Dev	0.3	12.0	0.0	0.0	0.0	271
COV	3%	2%	0%	0%	14%	37%

Table B39 IDT Results: RAP Content (Granite 15% RAP)

Specimen	Air Voids, %	Max Load, lbs	Displacement at Maximum Load, in.	Tensile Strength, psi
1	7.4	2311	0.13	98
2	7.3	1993	0.16	85
3	7.3	2150	0.13	91
4	6.9	2228	0.13	95
Average	7.2	2171	0.14	92
Std Dev	0.2	117	0.01	5
COV	3%	5%	8%	5%

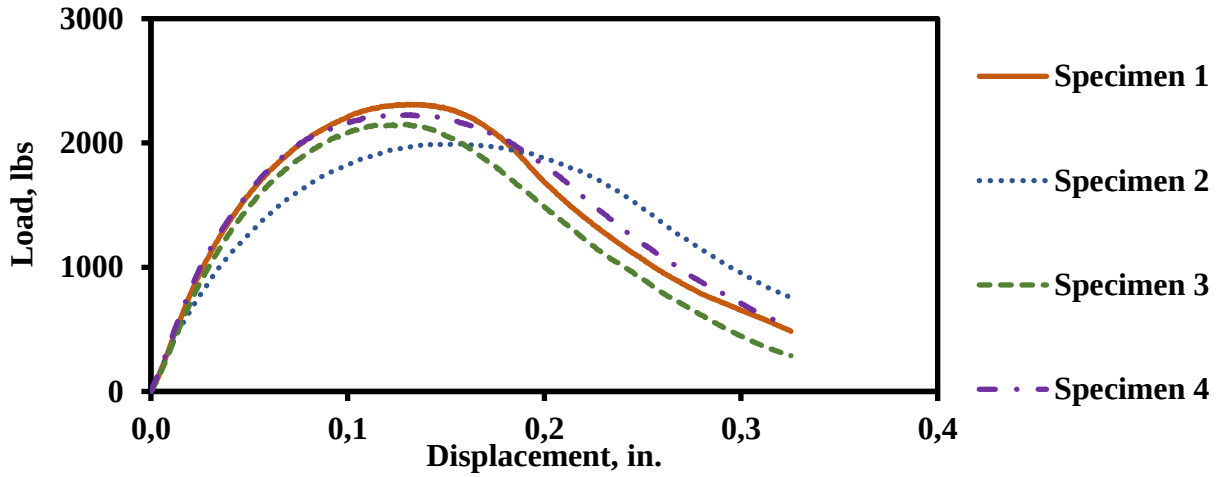

Figure B20 IDT results: RAP Content (Granite 15% RAP)

Table B40 OT Results: RAP Content (Granite 15% RAP)

Specimen	Air Voids, %	Max Load, lbs	Work of Fracture, in.-lbs	Critical Fracture Energy, in.-lbs/in.²	Crack Progression Rate	Number of Cycles to Failure
1	7.4	508.1	8.2	1.8	0.3	1000
2	7.5	574.8	8.9	2.0	0.4	582
3	7.9	494.7	6.8	1.5	0.4	315
4	7.3	486.8	7.2	1.6	0.3	1000
Average	7.5	516.1	7.7	1.7	0.3	724
Std Dev	0.2	34.7	0.8	0.2	0.0	291
COV	3%	7%	11%	11%	12%	40%

Table B41 IDT Results: RAP Content (Granite 30% RAP)

Specimen	Air Voids, %	Max Load, lbs	Displacement at Maximum Load, in.	Tensile Strength, psi
1	7.6	2555	0.11	108
2	7.2	2494	0.12	106
3	6.9	2623	0.13	111
Average	7.2	2558	0.12	109
Std Dev	0.3	53	0.01	2
COV	4%	2%	5%	2%

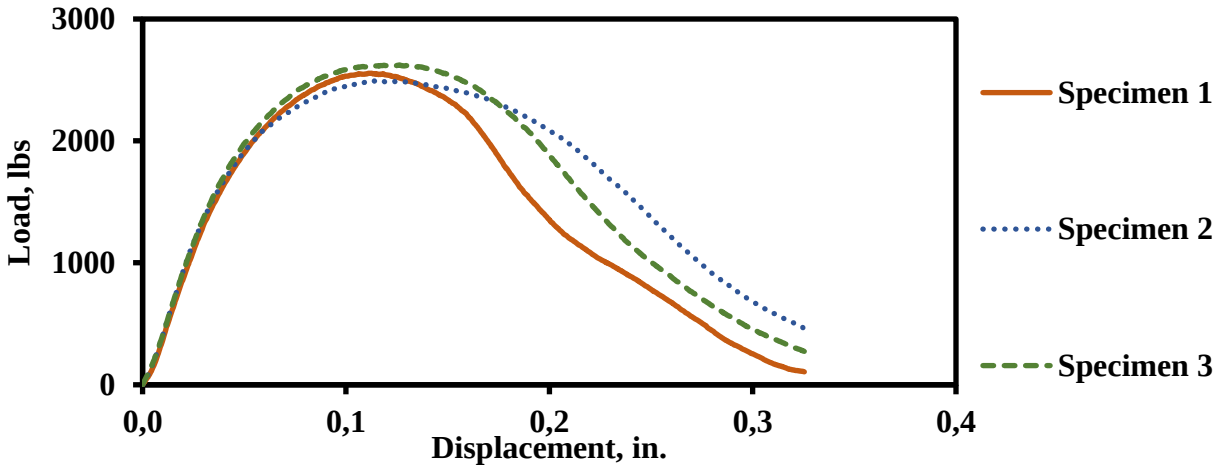

Figure B21 IDT results: RAP Content (Granite 30% RAP)

Table B42 OT Results: RAP Content (Granite 30% RAP)

Specimen	Air Voids, %	Max Load, lbs	Work of Fracture, in.-lbs	Critical Fracture Energy, in.-lbs/in.²	Crack Progression Rate	Number of Cycles to Failure
1	6.7	764.0	10.6	2.4	0.3	425
2	6.8	717.4	9.1	2.0	0.4	144
3	6.7	808.1	9.8	2.2	0.4	321
Average	6.7	763.2	9.8	2.2	0.4	297
Std Dev	0.0	37.0	0.6	0.1	0.0	116
COV	1%	5%	6%	6%	9%	39%

Table B43 IDT Results: RAP Content (Granite 45% RAP)

Specimen	Air Voids, %	Max Load, lbs	Displacement at Maximum Load, in.	Tensile Strength, psi
2	6.2	2689	0.15	114
3	6.7	2571	0.14	109
4	6.7	2459	0.14	104
Average	6.5	2573	0.14	109
Std Dev	0.2	94	0.01	4
COV	4%	4%	5%	4%

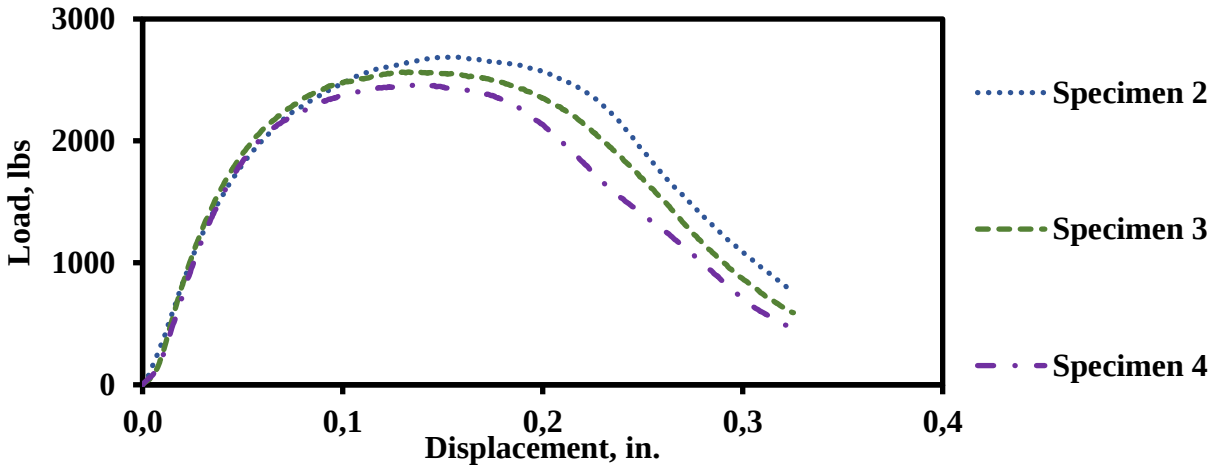

Figure B22 IDT results: RAP Content (Granite 45% RAP)

Table B44 OT Results: RAP Content (Granite 45% RAP)

Specimen	Air Voids, %	Max Load, lbs	Work of Fracture, in.-lbs	Critical Fracture Energy, in.-lbs/in.²	Crack Progression Rate	Number of Cycles to Failure
1	7.8	733.4	12.2	2.7	0.3	987
3	7.6	646.7	12.2	2.7	0.3	1000
4	8.0	690.7	8.6	1.9	0.4	249
Average	7.8	690.3	11.0	2.4	0.3	745
Std Dev	0.2	35.4	1.7	0.4	0.0	351
COV	2%	5%	15%	15%	13%	47%

Table B45 IDT Results: RAP Source (15% RAP Source B)

Specimen	Air Voids, %	Max Load, lbs	Displacement at Maximum Load, in.	Tensile Strength, psi
1	7.0	1743	0.13	74
2	6.3	2100	0.11	89
3	6.5	2098	0.11	89
4	6.0	1986	0.13	84
Average	6.5	1982	0.12	84
Std Dev	0.4	145	0.01	6
COV	6%	7%	9%	7%

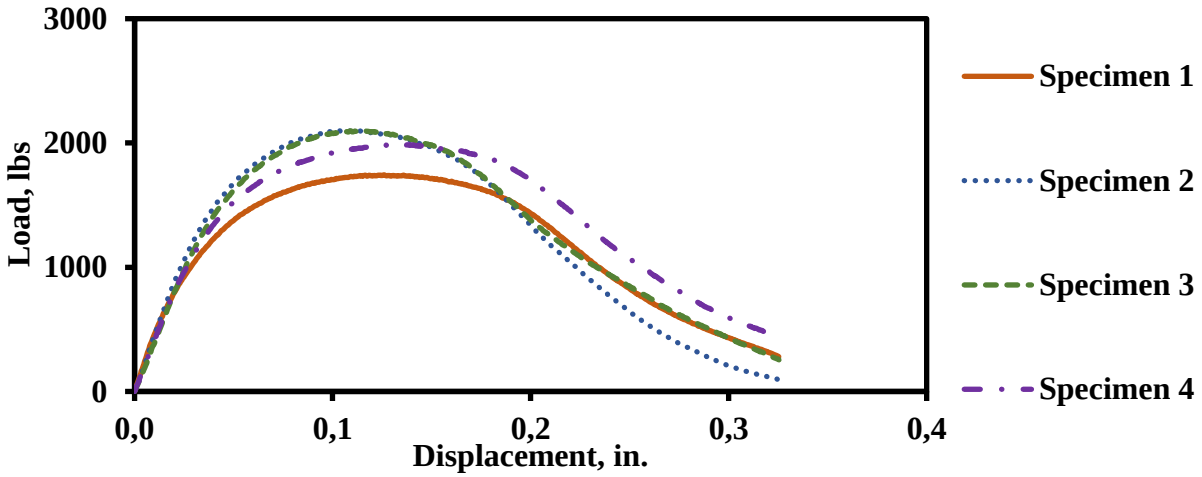

Figure B23 IDT results: RAP Source (15% RAP Source B)

Table B46 OT Results: RAP Content (15% RAP Source B)

Specimen	Air Voids, %	Max Load, lbs	Work of Fracture, in.-lbs	Critical Fracture Energy, in.-lbs/in.²	Crack Progression Rate	Number of Cycles to Failure
1	7.4	578.9	5.9	1.3	0.5	111
2	7.1	640.2	8.8	2.0	0.4	450
3	6.9	618.8	5.8	1.3	0.4	118
Average	7.1	612.6	6.8	1.5	0.4	226
Std Dev	0.2	25.4	1.4	0.3	0.0	158
COV	3%	4%	20%	20%	9%	70%

Table B47 IDT Results: RAP Source (30% RAP Source B)

Specimen	Air Voids, %	Max Load, lbs	Displacement at Maximum Load, in.	Tensile Strength, psi
1	7.1	2480	0.12	105
2	6.4	2707	0.11	115
3	7.2	2725	0.10	116
4	6.1	2540	0.13	108
Average	6.7	2613	0.11	111
Std Dev	0.5	105	0.01	4
COV	7%	4%	9%	4%

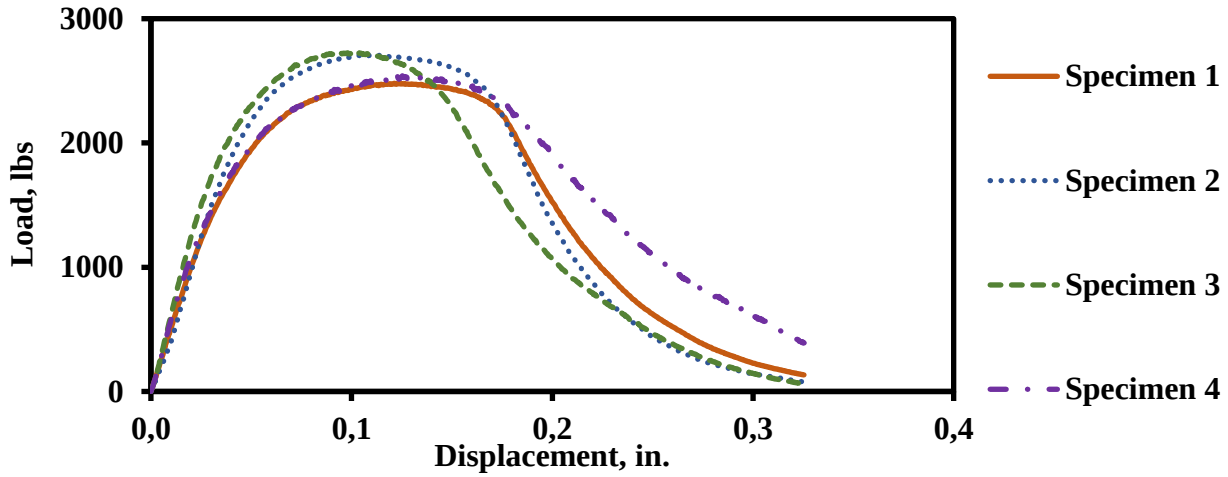

Figure B24 IDT results: RAP Source (30% RAP Source B)

Table B48 OT Results: RAP Content (30% RAP Source B)

Specimen	Air Voids, %	Max Load, lbs	Work of Fracture, in.-lbs	Critical Fracture Energy, in.-lbs/in.²	Crack Progression Rate	Number of Cycles to Failure
2	7.7	697.4	7.2	1.6	0.5	159
3	7.4	785.4	8.2	1.8	0.5	278
Average	7.6	741.4	7.7	1.7	0.5	219
Std Dev	0.2	44.0	0.5	0.1	0.0	60
COV	2%	6%	6%	6%	4%	27%

Table B49 IDT Results: RAP Source (45% RAP Source B)

Specimen	Air Voids, %	Max Load, lbs	Displacement at Maximum Load, in.	Tensile Strength, psi
1	6.4	2953	0.13	125
2	6.2	2994	0.14	127
3	6.2	2811	0.14	119
4	6.2	3000	0.16	127
Average	6.3	2940	0.14	125
Std Dev	0.1	76	0.01	3
COV	1%	3%	8%	3%

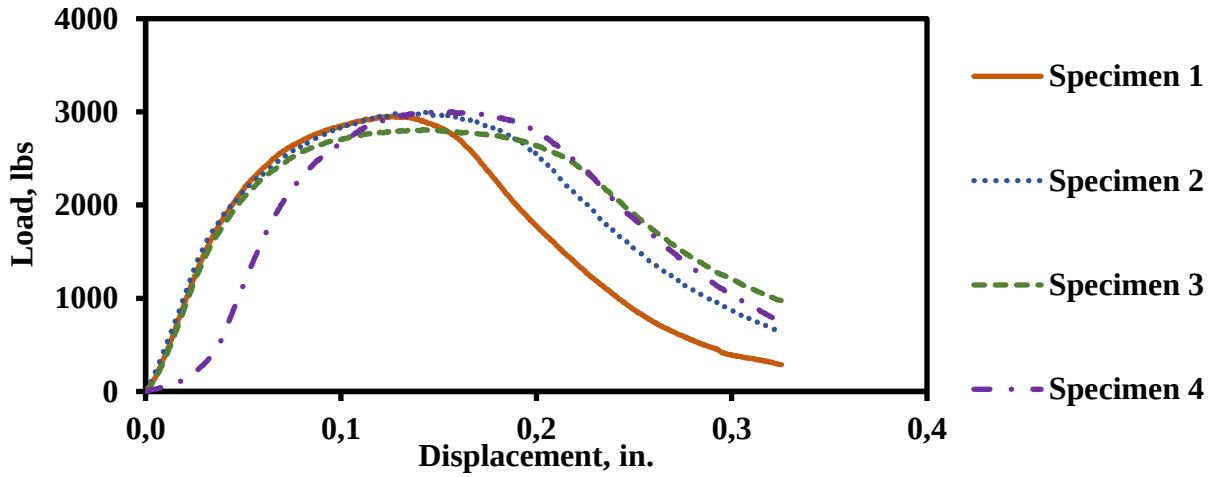

Figure B25 IDT results: RAP Source (45% RAP Source B)

Table B50 OT Results: RAP Content (45% RAP Source B)

Case	Air Voids, %	Max Load, lbs	Work of Fracture, in.-lbs	Critical Fracture Energy, in.-lbs/in.²	Crack Progression Rate	Number of Cycles to Failure
1	8.0	882.7	4.6		0.5	178
3	7.6	1111.9	11.3	2.5	0.7	55
4	7.7	786.7	4.9		0.7	85
Average	7.8	927.1	6.9	2.5	0.6	106
Std Dev	0.2	136.4	3.1	0.0	0.1	52
COV	2%	15%	45%	0%	13%	49%

Vita

Luiza Barros was born in Brazil where she spent most of her life. She received her Bachelors of Science in Civil Engineering from Pontific University Catholic of Minas Gerais in July 2015. To pursue her Bachelor's degree, Luiza Barros was fortunate to receive funding from the Program of University for All Scholarship (PROUNI), for five years (2010-2015). In summer 2015 she moved to United States to learn English and pursue her higher education. During the spring of 2016 she engaged in transportation research at a nationally recognized Center for Transportation Infrastructure Systems (CTIS) under prominent civil engineering researcher and mentor, Dr. Soheil Nazarian.

Ms. Barros completed a Master's Degree in Civil Engineering in August 2018. While a graduate student, she contribute and developed research projects for Texas Department of Transportation (TxDOT). She was awarded for an outstanding poster presentation with 2nd place at the UTEP Graduate Student Research Expo. She is a member of student organizations such as American Society of Civil Engineering (ASCE) and Transportation Leadership Council UTEP Chapter (TLC) in which she was a community representative officer in 2017. She was also a TLC fellow on the Transportation Research Board 96th Annual Meeting.

Contact Information: lhbarros@miners.utep.edu

This thesis was typed by Luiza Helena Barros.